Journal of Thermal Science Vol.31, No.6 (2022) 2088−2110

https://doi.org/10.1007/s11630-022-1676-8 **Article ID: 1003-2169(2022)06-2088-23**

Energy and Parameter Analysis of SOFC System for Hydrogen Production from Methane Steam Reforming

DENG Meilong, LIU Jinyi, ZHANG Xiaosong*, LI Jinsong, FU Lirong

School of Mechanics and Electronics Engineering, Hainan University, Haikou 570228, China

Abstract: In this paper, an integrated system of solid oxide fuel cell (SOFC) and methane steam reforming for hydrogen production is proposed. The mathematical model of the coupled integrated system is studied by COMSOL and Aspen software, and the energy analysis of the integrated system is carried out. The system recovers and reuses the waste heat of the SOFC stack through the heat exchanger, which can realize the cascade efficient use of energy. By adjusting the different reforming temperatures, steam-to-carbon ratio and SOFC operating temperature of methane steam reforming to produce hydrogen, the parameters that have a greater impact on the system are studied. The research results show that as the steam-to-carbon ratio and reformer operating temperature increase, the net output power and efficiency of the system increase. When the fuel cell operating temperature is 800°C, the output power and efficiency of the system reach the maximum values of 899.93 W and 52.52%, respectively. Increasing the operating temperature of SOFC helps to improve the efficiency of fuel cells, but the efficiency of the integrated system of methane steam reforming hydrogen production and SOFC first increases and then decreases. This system can realize the direct coupling between the SOFC reactor subsystem and the methane steam reforming hydrogen production system under optimized conditions, which has reference significance for the actual operating conditions of the coupled system.

Keywords: **SOFC, methane steam reformer, hydrogen, mathematical model, system optimization**

1. Introduction

With climate change and the growing global demand for energy, scholars all over the world are striving to find clean energy alternatives to fossil fuels in order to achieve high conversion efficiency. The fuel cell integrated system has become a very attractive power generation solution because it has high power, high efficiency, and no pollution to the environment. Many researchers have combined the solid oxide fuel cell (SOFC) and traditional thermal cycle into an integrated system, which has become a valuable tool for studying integrated system technology. This method can recover the heat energy of the SOFC and use it to improve the efficiency of the fuel cell, and determine the best configuration and conditions of the integrated system [1, 2].

The efficiency of the traditional SOFC system is 48%–53% [3–6]. Many scholars have put forward the concept of a SOFC integrated system to improve the efficiency of SOFC [7]. In the new fuel cell integrated system, the combination of SOFC and gas turbine (GT) is considered to be the best integrated system technology in the current integrated system due to the fuel flexibility and high efficiency of the integrated system [8–10].

Received: Mar 21, 2022 AE: LI Yinshi Corresponding author: ZHANG Xiaosong E-mail: zhangxiaosong@hainanu.edu.cn

Nomenclature

A_{cell}	Active area/m^2
F	Faraday Constant
ΔG	Gibbs free energy/kJ·kg^{-1}
I	Current/A
i	Current density/A·m^{-2}
i_0	Exchange current density/A·m^{-2}
m_{CH_4}	Methane flow in reformer/mol·s^{-1}
N_{cell}	Number of cell
n_e	Number of electrons
W	Power/W
p	Pressure/Pa
Q_{loss}	Heat loss/W
R	Resistance/Ω
R_g	Universal gas constant/J·(mol·K)$^{-1}$
T	Temperature/°C
V_{act}	Activation overvoltage/V
V_{conc}	Concentration overvoltage/V
V_{ohm}	Ohmic overvoltage/V
V_{act}	activation energy/J·mol^{-1}
V^0	Open circuit voltage/V
V_{cell}	SOFC stack voltage/V
W	Power/W
X_{CH_4}	Methane conversion rate/%

Greeks

ε	Porosity
η	Efficiency/%
η_p	Blower efficiency/%
σ	Charged-species conductivity/S·m^{-1}

Abbreviations

AC	Air compressor
AB	After burner
CHP	Cooling heating and power
ER	External reformer
FC	Fuel compressor
GT	Gas turbine
HEX1	Heat exchanger 1
HEX2	Heat exchanger 2
HEX3	Heat exchanger 3
IR	Internal reformer
KC	Kalina cycle
LHV	Lower heating value
MX	Mixer
ORC	Organic Rankine Cycle
SR	Steam reformer
SOFC	Solid oxide fuel cell
WP	Water pump

Many researchers have conducted theoretical analysis and simulation research on the SCOFC-GT system. In the SOFC-GT integrated system, GT is used to recover the waste heat of the SOFC, and the waste heat of the gas turbine can be recovered by other methods, which can fully improve the energy conversion efficiency of the integrated system. Yingru Zhao et al. [11] proposed a new type of SOFC-GT hybrid power system, which recovers the waste heat of GT for preheating fuel gas and air. The results show that the power generation scale of the proposed new integrated system is 2000–2500 W/m^2, and the efficiency varies between 50% and 60%.

Some scholars proposed multi-generation integrated systems based on SOFC-GT to improve the efficiency of the system [12–14]. Singh and Singh [15] proposed an Organic Rankine Cycle (ORC) integrated system based on SOFC-GT (SOFC-GT-ORC) and performed a thermodynamic analysis. The results show that the efficiency of the SOFC-GT-ORC integrated system is increased to 75.81%, which is 2% higher than that of the traditional SOFC-GT integrated system. Wang et al. [16] analyzed a new type of SOFC-GT-Kalina cycle (SOFC-GT-KC) power generation system from the perspective of the first and second laws of thermodynamics. This new integrated system uses KC to recover the waste heat of SOFC-GT to improve overall performance. The study also shows that the electrical efficiency of the SOFC-GT-KC integrated system is 67%. Akkaya and Sahin [17] proposed a new SOFC-ORC integrated system, and the results show that the efficiency of the new integrated system is 14% higher than that of a single SOFC. Eisevi et al. [18] proposed different SOFC-GT integrated power generation systems with internal reformer hydrogen production devices. The simulation results using EES software show that the series SOFC-GT is more efficient than the traditional SOFC-GT and parallel SOFC-GT. Moradi et al. [19] used MATLAB software to study an energy system centered on SOFC, which is composed of fuel cells, solar parabolic disk collectors, ORC and absorption refrigeration systems. The results show that the overall efficiency of the system is 49%. The integration of SOFC-GT-VARS-ORC is studied by Pranjal Kumar [20]. In this system, SOFC-GT combined with thermodynamic analysis, vapor absorption refrigeration system (VARS) combined with a steam turbine to achieve the cooling effect; ORC uses the heat carried by the exhaust gas in the system to generate electricity. The results show that compared with the efficiency of the traditional SOFC-GT integrated system, the efficiency of the new integrated

system has increased from 58.88% to 68.79%. Mehdi Mehrpooya [21] proposed a combined cooling, heating and power (CCHP) generation system based on SOFC technology. Simulation results using Aspen Plus show that the cooling efficiency of the SOFC-CCHP integrated system reaches 58%, and the total electrical efficiency of the CCHP system reaches nearly 60%. Zhang Qinwei et al. [22] proposed a new power generation system combining chemical chain hydrogen production with SOFC. Simulation results using Aspen Plus show that compared with the SOFC reforming system, the new integrated system's power generation efficiency can reach 61.2%, and the relative efficiency of the production system is increased by about 18%. System modeling based on commercial software can be effectively simulated, but the use of commercial software requires extensive knowledge of programming skills. Therefore, the existing commercial software has some limitations.

At present, due to the high operating temperature of SOFC and its insensitivity to CO toxicity and the wide use of fuels, the use of methane fuel in SOFC to produce hydrogen is a typical method, while the main methods of using methane to produce hydrogen in SOFC are internal reforming and external reforming [23]. External reforming is to send methane fuel to the reformer for reforming reaction to produce H_2 and CO and other gases, and then send the reformed fuel gas to the SOFC system for electrochemical reaction with air to generate electricity; internal reforming is to pass methane directly into the anode catalyst layer of SOFC for reforming reaction. Internal reforming can effectively couple the transfer of material and energy, reduce the cooling requirements of the fuel cell stack, and improve energy utilization and system efficiency [24]. The electrochemical reaction in the internal reforming solid oxide fuel cell produces water, which can provide a cold cut for the fuel cell, reducing the flow of air into the cathode side of the fuel cell, thereby reducing the power consumed by the air compressor. However, in the actual operation process, the direct internal reforming method will quickly absorb heat at the fuel inlet, causing the temperature gradient of the entire fuel cell stack to increase, causing the anode and electrolyte materials to rupture, so the life of the fuel cell is greatly shortened [25]. In addition, internal reforming will deposit nickel on the surface of the catalyst [26], which reduces the active sites of the catalyst layer, resulting in a poor reforming effect, thereby reducing the power generation efficiency of the fuel cell. The external reforming technology is more mature than the internal reforming technology, which can effectively avoid carbon deposition on the anode catalyst layer of the fuel cell and ensure the stability of the reformer reaction [27].

To alleviate the above-mentioned problems faced by SOFC internal reforming, an external reformer can be used to convert methane into fuel gas such as H_2, which is then fed to the anode side of the SOFC. Since the endothermic reforming reaction and the exothermic electrochemical reaction are carried out separately in different devices, the system efficiency of hydrogen production using external reforming in SOFC is lower than that of internal reforming, but it has some characteristics worth considering. The external reforming reaction can not only produce hydrogen with the required concentration of SOFC but also produce high-temperature exhaust gas to improve the efficiency of the system [28]. Saebea et al. [29] analyzed the performance of SOFC external reforming, which integrated an external biogas reformer. The results show that the system using ethanol as fuel in the external reforming of SOFC has the highest electrical and thermal efficiency. Farhad et al. [30] compared the effects of three different methods (anode outlet gas recirculation, steam reforming, and partial oxidation) on the electrical efficiency of SOFC combined heat and power (CHP) systems. The results show that the integrated system that recovers and recycles the exhaust gas from the anode outlet has the highest electrical efficiency, followed by steam reforming, and the lowest efficiency is partial oxidation.

In this paper, a SOFC and methane steam reforming hydrogen production integrated system is proposed. Compared with other SOFC systems that carry external reforming hydrogen production [31–37], the overall structure of the system proposed in this study is more compact, and the installation size and occupied volume are further reduced and low cost. The integrated system proposed in this paper is mainly composed of SOFC, external reforming hydrogen production and other auxiliary equipment. The hydrogen produced by the steam reforming of methane is fed into the SOFC, and the heat required by the steam reformer is provided by the high-temperature gas generated after the incompletely reacted gas of the SOFC is combusted in the afterburner. The integrated system was studied using COMSOL and Aspen software, and the key mathematical models (SOFC and reformer) in the integrated system of SOFC and methane steam reforming for hydrogen production were verified to ensure that the proposed integrated system could accurately predict the system's performance. In addition, the energy analysis method is used to analyze the integrated system. In the system, energy analysis is performed according to the enthalpy value of the system to determine the heat loss of the entire system. Finally, a parametric study of the integrated system of SOFC and methane steam reforming for hydrogen production is carried out to determine the optimal operating parameters of the integrated system.

2. Description of SOFC Combined with Methane Reforming Hydrogen Production System

In this research, a SOFC integrated system for hydrogen production by external reforming is proposed. In this integrated system, the SOFC and the external reforming hydrogen production unit are simulated using COMSOL Multiphysics 5.6, while the other subsystems are simulated using Aspen Plus V9.0. To analyze the performance of the proposed system, the mass and energy balance equations of the system should be recorded according to the first and second laws of thermodynamics [38].

In SOFC, the exhaust gas discharged from the cathode and anode retains high-quality energy, which accounts for about 35% of the heat energy in the unreacted fuel and exhaust gas [39]. The incompletely reacted fuel is burned in the afterburner to use this part of the heat energy to improve the efficiency of the entire system. The system includes a SOFC stack, external reforming, combustor, three heat exchangers, an air compressor, fuel compressor, mixer and water pump. The fuel uses an external reformer to produce hydrogen, and the energy used to convert methane fuel is provided by the waste heat in the afterburner. Fig. 1 shows a schematic diagram of an integrated power generation system based on SOFC. In the sub-system of the methane steam reforming reaction, the methane and steam preheated by the heat exchanger are transported to the reformer, where an endothermic reaction occurs and syngas composed of CH_4, H_2O, H_2 and CO_2 is produced. The high-temperature exhaust gas generated in the afterburner provides the required reaction heat. The operating temperature is 729°C and the pressure is 101.32 kPa. In the SOFC subsystem, the operating temperature of the SOFC is 800°C; the pressure is atmospheric; the anode side is fed with synthetic gas produced by the methane steam reforming reaction, and the cathode side is fed with air and nitrogen. In the system block diagram, this study only considers the system performance in the dashed block diagram, and does not consider the system performance outside the dashed line.

The air for the fuel cell cathode is provided by an air compressor (AC). The air is pressurized by an air compressor and then heated in a heat exchanger 3 (HEX3) before being fed into the cathode channels of the SOFC stack. The air temperature provided by the AC is relatively lower than the operating temperature of the SOFC to cool the fuel cell stack. The ratio of steam to carbon is defined as the ratio of the molar flow rates of steam and methane, and the S/C is set to 2.5. The pressure of methane and water is slightly increased by the fuel compressor (FC) and the water pump (WP) to the operating pressure of the fuel cell, and the exhaust gas passing through the post combustion chamber is heated in the heat exchanger 2 (HEX2) and heat exchanger 1 (HEX1) to the temperature required by the fuel cell. The pressurized and heated steam and fuel are mixed in a mixer (MX). The mixed gas is fed into an external reformer (steam reformer, SR) for reforming reaction and water gas shift reaction. The hydrogen produced by the reforming reaction is sent to the anode side of the SOFC, where it electrochemically reacts with the oxygen in the cathode air to generate a direct current. The inverter is used to convert the direct current generated by the fuel cell stack into alternating current. After the

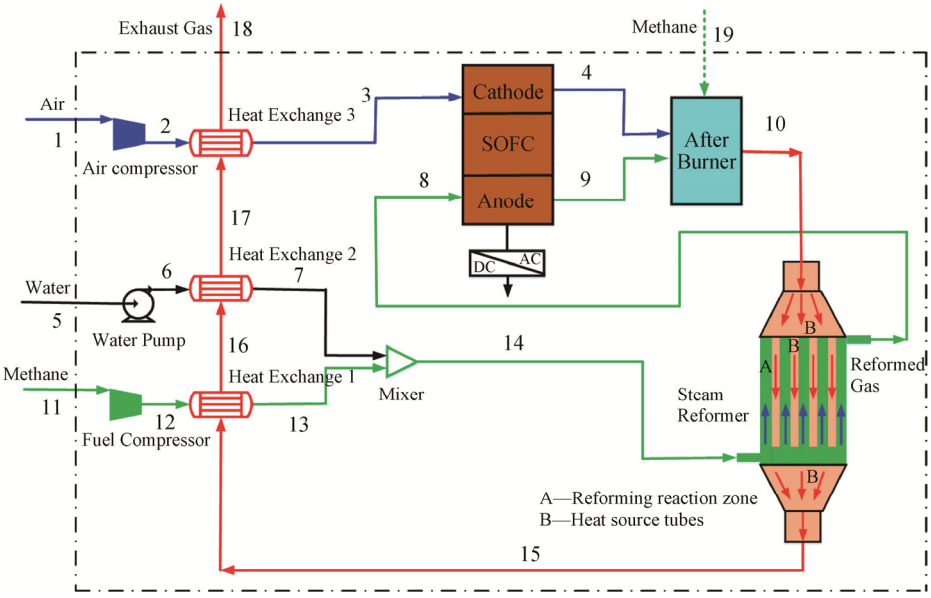

Fig. 1 Schematic diagram of a combined SOFC and methane steam reforming hydrogen production system

electrochemical reaction occurs in the SOFC, the incompletely reacted fuel and the cathode remove excess air, and enter the afterburner chamber (AB) to completely burn to produce high-temperature gas. Assume that the remaining fuel at the anode and the excess air at the cathode in the SOFC is completely combusted in the afterburner to generate a large amount of heat energy. A part of the heat energy in the exhaust gas of the afterburner chamber is used in the reforming reactor to provide heat energy for the steam reforming reaction. The other part of the heat energy is the air fed into the cathode side of the SOFC to be heated by the heat exchanger 3 (HEX3). In the reformer, the high-temperature exhaust gas generated after the strong endothermic reforming reaction and the weakly exothermic water gas shift reaction is used to heat water into steam and heat methane through the HEX1 and the HEX2, respectively. For the SOFC operating temperature to be relatively high, additional fuel must be provided to burn in the AB chamber to generate heat energy to heat the air on the cathode side of the fuel cell to reach the operating temperature of the SOFC.

3. Mathematical Model Description of SOFC Integrated System

In this section, the various subsystems of the system are described, but experimental results published by other researchers are cited to verify the simulation reliability of key subsystems such as SOFC and reformer, and therefore provide a reliable basis for the next chapter.

3.1 Description of SOFC mathematical model

3.1.1 Electrochemical reaction

The geometrical dimensions, physical parameters and operating conditions of the SOFC establish a mathematical model, as shown in Table 1. The electrolyte material used in the established SOFC model is Y_2O_3-stabilized ZrO_2 (YSZ). The anode and cathode materials of SOFC are nickel cermet and lanthanum manganate, respectively [40, 41]. The research of the SOFC model is carried out under thermodynamic equilibrium and steady-state conditions. The model mainly includes electrochemical reaction models and thermodynamic models based on mass conservation equations and energy conservation equations. In addition, due to the relatively small changes in kinetic energy and potential energy, it is usually not considered when analyzing the model. In the SOFC subsystem, some assumptions are adopted to simplify the analysis of this subsystem as follows [16, 42–45]:

(1) Air is mainly composed of 21% O_2 and 79% N_2 per volume fraction;

(2) In SOFC, the anode and cathode pressures are considered constant and equal;

Table 1 Parameter setting in SOFC simulation

Parameter	Value	Unit
Cell length	10	mm
Gas channel width	0.5	
Electrode thickness	0.1	
Rib width	0.5	
Membrane thickness	0.1	
Gas channel height	0.5	
Porosity of anode	30%	–
Porosity of cathode	30%	–
Cathode Exchange current density	0.1	A/m^2
Anode exchange current density	0.3	
Anode electrode conductivity, σ_a	$\sigma_a = \frac{4.2\times10^7}{T}\exp\left(-\frac{1200}{T}\right)$	S/m
Membrane conductivity, σ_m	$\sigma_m = 33.4\times10^3\exp\left(-\frac{10.3\times10^3}{T}\right)$	
Cathode electrical conductivity, σ_c	$\sigma_c = \frac{9.5\times10^7}{T}\exp\left(-\frac{1150}{T}\right)$	

(3) Contact resistances are negligible;

(4) All gases and fuels are ideal gases;

(5) The exhaust gas that does not participate in the electrochemical reaction in the SOFC subsystem is completely burned in the afterburner to produce high-temperature gas;

(6) The operating temperature of the SOFC is equal to the temperature of the gas at the anode and cathode outlets;

(7) The SOFC subsystem is in a steady-state system, and the electrochemical reaction reaches an equilibrium state;

(8) At the anode of the SOFC, only hydrogen undergoes an electrochemical reaction;

(9) The cell stack composed of each cell always provides hydrogen and air.

In SOFC, hydrogen and oxygen undergo an electrochemical reaction to generate electricity. The reduction reaction that occurs on the cathode electrode side generates oxygen ions, and the oxidation reaction that occurs on the anode electrode side generates steam and electrons. The specific electrochemical reaction is as follows:

Anode: $H_2+O^{2-} \rightarrow H_2O+2e^-$

Cathode: $O_2+4e^- \rightarrow 2O^{2-}$

Overall reaction: $2H_2+O_2 \rightarrow 2H_2O$

In SOFC, when the current density is given, the voltage can be determined, and the performance of the SOFC can be characterized by the actual cell voltage. The actual output cell voltage of the SOFC is always less

than the open-circuit voltage. Because the three main losses encountered in the actual operation of SOFC are ohmic over-potential, anode and cathode activation over-potential, and anode and cathode concentration over-potential.

The reversible voltage of SOFC can be calculated using the Nernst equation [46]:

$$E_{\mathrm{r}} = E^0 + \frac{R_{\mathrm{g}}T}{n_{\mathrm{e}}F}\ln\left(\frac{p_{\mathrm{H_2}} \cdot p_{\mathrm{O_2}}^{1/2}}{p_{\mathrm{H_2O}}}\right) \tag{1}$$

where R_{g} is the gas constant (8.314 J/(mol·K)); n_{e} is the number of electrons(n_{e}=2); F is the Faraday constant; T is the operating temperature of the SOTC; $p_{\mathrm{H_2}}$, $p_{\mathrm{H_2O}}$, $p_{\mathrm{O_2}}$ are partial pressures of H_2, H_2O and O_2, respectively (kPa), and V^0 is reversible open-circuit voltage under standard temperature and pressure conditions (V). The standard reversible open-circuit voltage can be calculated by the following formula:

$$E^0 = 1.253 - 2.4516\times10^{-4}T \tag{2}$$

Due to internal resistance and overvoltage loss, the actual output voltage of the SOFC is lower than the open-circuit voltage. The actual voltage generated by the SOFC stack can be defined as:

$$V_{\mathrm{out}} = V_{\mathrm{r}} - V_{\mathrm{act}} - V_{\mathrm{ohm}} - V_{\mathrm{con}} \tag{3}$$

where V_{out}, V_{act}, V_{ohm} and V_{con} are cell actual voltage, the activation overvoltage, ohmic overvoltage and concentration overvoltage, respectively.

The local current density of the SOFC stack is calculated from the Butler-Volmer equation [47]:

$$i_{\mathrm{an}} = i_{0,\mathrm{an}}\left\{\exp\left(\frac{\alpha n_{\mathrm{e}}F V_{\mathrm{an,act}}}{R_{\mathrm{g}}T}\right) - \exp\left[-(1-\alpha)\frac{n_{\mathrm{e}}F V_{\mathrm{an,act}}}{R_{\mathrm{g}}T}\right]\right\} \tag{4}$$

$$i_{\mathrm{ca}} = i_{0,\mathrm{ca}}\left\{\exp\left(\frac{\alpha n_{\mathrm{e}}F V_{\mathrm{ca,act}}}{R_{\mathrm{g}}T}\right) - \exp\left[-(1-\alpha)\frac{n_{\mathrm{e}}F V_{\mathrm{ca,act}}}{R_{\mathrm{g}}T}\right]\right\} \tag{5}$$

where i_0 is the exchange current density; i is the current density; α is the charge transfer coefficient, which is between 0 and 1. The electrode exchange current density proposed by Aguiar et al. [5] is a function of activation energy, fuel cell operating temperature and pre-exponential factor. The specific calculation is as follows:

$$i_{0,\mathrm{an}} = \frac{R_{\mathrm{g}}T}{nF}K_{\mathrm{anode}}\exp\left(-\frac{E_{\mathrm{anode}}}{R_{\mathrm{g}}T}\right) \tag{6}$$

$$i_{0,\mathrm{ca}} = \frac{R_{\mathrm{g}}T}{nF}K_{\mathrm{cathode}}\exp\left(-\frac{E_{\mathrm{cathode}}}{R_{\mathrm{g}}T}\right) \tag{7}$$

The values of the pre-exponential factor and activation energy for calculating the current density are listed in Table 2.

Table 2 Specific values of pre-exponential factor and activation energy

Parameters	Value	Unite
K_{anode}	6.54×10^{11}	$1/(\Omega\cdot m^2)$
K_{cathode}	2.35×10^{11}	
E_{anode}	140	kJ/mol
E_{cathode}	137	

The flow of electrons through the electrode and the flow of ions through the electrolyte cause Ohmic loss, which is estimated according to Ohm's law. The calculation of Ohm's law is as follows [48–50]:

$$V_{\mathrm{ohm}} = iR_{\mathrm{ohm}} = i\left(R_{\mathrm{ion}} + R_{\mathrm{elec}} + R_{\mathrm{con}}\right) \tag{8}$$

where R_{ohm} is the total resistance; R_{ion}, R_{elec}, R_{con} are ionic resistance, electronic resistance and contact resistance, respectively.

Concentration overvoltage can be calculated by the following equation [51–54]:

$$V_{\mathrm{con}} = V_{\mathrm{con,a}} + V_{\mathrm{con,c}} = \frac{R_{\mathrm{g}}T}{2\mathrm{F}}\ln\left(\frac{p_{\mathrm{H_2}}p_{\mathrm{H_2O}}^0}{p_{\mathrm{H_2O}}p_{\mathrm{H_2}}^0}\right) + \frac{R_{\mathrm{g}}T}{4\mathrm{F}}\ln\left(\frac{p_{\mathrm{O_2}}}{p_{\mathrm{O_2}}^0}\right) \tag{9}$$

where p^0 is the pressure of various substances in the standard state.

Activation polarization, also known as electrochemical polarization, is the reaction resistance of activation energy that must be overcome for electrochemical reactions [55–57].

$$\eta_{\mathrm{act}} = \eta_{\mathrm{act,a}} + \eta_{\mathrm{act,c}} = \frac{R_{\mathrm{g}}T}{2\alpha\mathrm{F}}\sin h^{-1}\left(\frac{i_{\mathrm{an}}}{2i_{\mathrm{an},0}}\right) + \frac{R_{\mathrm{g}}T}{4\alpha\mathrm{F}}\sin h^{-1}\left(\frac{i_{\mathrm{ca}}}{2i_{\mathrm{ca},0}}\right) \tag{10}$$

Current density is one of the key parameters for evaluating the performance of fuel cell stacks. The current density can be expressed by Faraday's law [58, 59]:

$$i = \frac{n_{\mathrm{e}}\mathrm{F}z_{\mathrm{r}}}{N_{\mathrm{cell}}A_{\mathrm{cell}}} \tag{11}$$

where N_{cell} is the number of SOFC stacks composed of single cells. A_{cell} is the active area of the cell; z_{r} is the extent of electrochemical reaction, mol/s.

The current expression of the fuel cell can be expressed by the following formula:

$$I = i \cdot A_{\mathrm{cell}} \tag{12}$$

The output power of the SOFC stack is given by:

$$W_{\mathrm{SOFC}} = I \cdot V_{\mathrm{out}} \cdot N_{\mathrm{cell}} \tag{13}$$

The electrical efficiency of SOFC can be defined as:

$$\eta_{\mathrm{SOFC}} = \frac{W_{\mathrm{SOFC}}}{n_{\mathrm{fuel}} \cdot \mathrm{LHV}} \tag{14}$$

where m_{fuel} is the molar flow rate of the fuel; LHV is the low heating value of the fuel.

The mass conservation equation and energy conservation equation of fuel cells consider the anode channel and cathode channel, as well as the change of gas composition and gas specific heat with temperature caused by electrochemical reaction. The heat loss can be derived from the energy balance equation:

$$m_3 h_3 + m_8 h_8 = m_4 h_4 + m_9 h_9 + W_{\mathrm{SOFC}} + Q_{\mathrm{loss,SOFC}} \tag{15}$$

where h_i is the enthalpy at the inlet and outlet of the fuel cell (kJ/mol); m_i is the molar flow rate (mol/s). $Q_{\mathrm{loss,SOFC}}$ is the heat loss of the SOFC (kJ/s).

3.1.2 Mesh analysis of SOFC model

The geometric shape of SOFC varies greatly in the directions of the *x*-axis and *y*-axis, so the number of meshes and their geometric shapes are very sensitive to the calculation of the convergence of the nonlinear governing equations involved in the model using COMSOL. Since the electrochemical reaction of SOFC is in the catalyst layer, the concentration distribution of the reaction gas and the current density will change, so the geometric mesh distribution in the *z*-direction of the two electrodes is realized with a higher mesh density. The schematic diagram of SOFC model meshing is shown in Fig. 2. The boundary layer is used to control the edge cells in the mesh in the *y*-axis direction of the collector surface, and the edge cells are used to control the mesh in the *z*-axis direction of the gas channels, electrodes, and polymer membrane. Then, a 3-dimension mesh is constructed in the entire SOFC computing domain in the form of a swept mesh from the *y*-*z* plane-level source surface along the *x*-direction to the target surface.

Analyzing the mesh is the SOFC model to generate a stable mesh to verify that the results of the simulation have nothing to do with the mesh structure and size. The mesh analysis is achieved by changing the density of the original mesh on the *z*-axis height position of each component of the SOFC. Table 3 shows the specifications of coarse mesh, fine mesh and extra-fine mesh. After calculating the results of three kinds of mesh, coarse, refined and ultra-fine, it is found that the calculation time of coarse mesh is the lowest among the three mesh types, but it overestimates the current density by more than 8.7%. When using the refined mesh to calculate, it is found that the error of the current density is less than 2.8%, which indicates that the simulation result of the SOFC model does not change greatly with the change of the mesh density. Because the convergence time of the SOFC model calculation will not increase significantly with the refinement of the mesh, the final mesh is selected as the ultra-fine mesh as the calculation mesh of the SOFC model to provide good accuracy in a reasonable time.

3.1.3 Validation of the SOFC model

For the fuel cell model, the simulation results are compared with the experimental data of Mohsen Sadeghi [60]. The experimental data of Mohsen Sadeghi is used to verify the three-dimensional model of the SOFC in this paper. The geometric participation and flow field types in the SOFC model are similar to the parameters in the experiment. Under the same operating conditions, if the experimental performance of the SOFC reactor is similar to the simulated performance, it can be

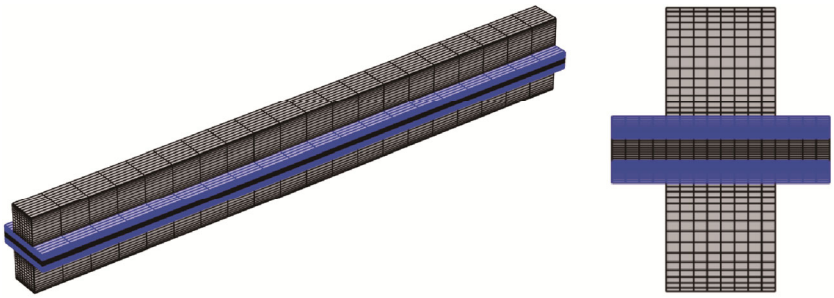

Fig. 2 Mesh geometry model of the SOFC model

Table 3 The number of mesh layers along with the thickness of the component

Parameter	The number of mesh layers along the *z*-axis of the component			Total number of mesh
	Gas diffusion layer	Electrode	Membrane	
Coarse mesh	2	3	3	16 981
Refined mesh	4	5	5	28 820
Ultra-fine mesh	7	9	9	31 796

considered that the three-dimensional SOFC model developed and established can reflect the actual operating conditions. Fig. 3 shows the comparison of the SOFC polarization curve with the polarization curve obtained from the experimental data in Ref. [60]. The operating temperature and pressure of the SOFC model and experiment are both at 800°C and 101.32 kPa, and the error between the obtained simulation data and the experimental results is very small. The current densities corresponding to the experimental results and simulation results at a voltage of 0.65 V are 0.64 W/cm^2 and 0.71 W/cm^2, respectively. By changing the operating temperature and reactant concentration in the SOFC model, the electrochemical loss caused by the electrochemical reaction is reduced, so that the model can better match the experimental results. The relative deviation between the polarization curve obtained by the SOFC model and the experimental result is less than 2.58%. Therefore, it can be concluded that the SOFC model established in this paper is reasonable and can be used to study the actual fuel cell operating status.

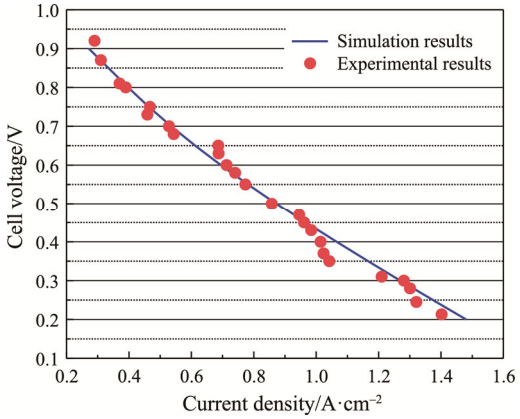

Fig. 3 Comparison of polarization curves between simulation and experimental results

3.2 Description of the methane steam reformer model

3.2.1 Methane steam reformer description

In the fuel cell, the steam reformer device usually provides the required hydrogen for the stack. In this article, the geometry of the methane steam reformer device is cylindrical, and the model is reduced to a quarter of the entire geometry by using symmetry for simulation calculations. Table 4 shows the geometric parameters of the methane steam reformer. The reformer is composed of a catalytic bed, a heating tube and an insulating jacket. In the model, methane is used as fuel gas, and water vapor is used as supporting gas. The methane steam reforming reaction is carried out on the Ni/Al_2O_3 catalyst [61]. The reference pressure is the atmospheric pressure state. The inlet temperature of the catalytic bed and heating tube are 729°C and 537°C, respectively. The chemical reaction process of methane in the steam reformer is modeled using COMSOL Multiphysics 5.6 software. In the reformer simulation process, only the overall oxidation of hydrogen is considered; that is, only the hydrogen undergoes an electrochemical reaction, does CO generate hydrogen through a water gas shift reaction, and at the same time, does methane generate hydrogen through a reforming reaction.

Table 4 Geometric and input parameter settings in the reformer model

Parameter	Value	Unite
Total length	150	mm
Catalytic bed radius	30	
Insulation jacket radius	33	
Heating tube radius	0. 4	
Reforming bed thermal conductivity	0.3	W/(m·K)
Jacket thermal conductivity	0.027	W/(m·K)
Density	3960	kg/m^3
Heat capacity	2800	J/(kg·K)
Catalytic bed porosity	0.3	–
Heat transfer coefficient of the heating tube	200	W/(m^2·K)
Reformer bed heat transfer coefficient	2	W/(m^2·K)
Heating tube inlet speed	3	m/s
Reformer bed permeability	10^{-9}	m^2
Inlet gas composition	42% CH_4 and 58% H_2O	–

Basic simplification and assumptions are as follows:

(1) Considering the repeatability of the reformer unit, only take 1/4 of the geometric shape for analysis;

(2) The methane and water vapor at the inlet of the reforming bed are fully mixed and treated as an ideal gas;

(3) The effect of coke formation caused by methane decomposition in the reaction on the activity of the catalyst is not considered.

In the SOFC hybrid system, an external reformer is used to convert methane into hydrogen required for fuel cell operation. Usually, steam is added to the external reformer to promote the reforming reaction, which can prevent the CO from cracking and prevent the coke deposits in the reformer from being harmful to the fuel cell catalyst layer. The heat required for the reforming reaction is provided by the exhaust gas discharged from the afterburner. Since the exhaust gas recovered from the afterburner contains a certain amount of oxygen, there are mainly oxidation reactions and steam reforming of

methane in the reformer, but the reforming reaction of methane is mainly considered. According to the Gibbs free energy thermodynamic equilibrium reaction, the steam reforming reaction model is established. The main reactions considered are the strongly endothermic methane steam reforming reaction and the weakly exothermic water gas shift reaction, both of which are reversible reactions, shown as follows:

Methane and water reforming reaction:

$$CH_4 + H_2O \leftrightarrow CO + 3H_2 \qquad \Delta H = +206 \text{ kJ/mol}$$

Water-gas shift reaction:

$$CO + H_2O \leftrightarrow CO_2 + H_2 \qquad \Delta H = -41 \text{ kJ/mol}$$

Total reaction:

$$CH_4 + 2H_2O \leftrightarrow CO_2 + 4H_2 \qquad \Delta H = +165 \text{ kJ/mol}$$

According to the reaction equation, the hydrogen outlet flow rate in the reformer can be obtained as follows:

$$m_{H_2,out} = m_{H_2,in} + m_{CO,eq} + 3m_{CH_4,eq} \tag{16}$$

where, $m_{H_2,in}$ and $m_{H_2,out}$ represent the molar flow rate of hydrogen at the outlet and inlet of the reformer, respectively (mol/s); $m_{co,eq}$ and $m_{CH_4,eq}$ are the equilibrium conditions for the flow rates of carbon monoxide and methane, respectively (mol/s).

The specific kinetic model and parameters are as follows [62]:

$$r_1 = \frac{k_1}{p_{H_2}^{2.5}}\left(p_{CH_4}p_{H_2O} - \frac{p_{CO}p_{H_2}^3}{K_1}\right)\Big/\text{DEN}^2 \tag{17}$$

$$r_2 = \frac{k_2}{p_{H_2}}\left(p_{CO}p_{H_2O} - \frac{p_{CO_2}p_{H_2}}{K_2}\right)\Big/\text{DEN}^2 \tag{18}$$

$$r_3 = \frac{k_3}{p_{H_2}^{3.5}}\left(p_{CH_4}p_{H_2O}^2 - \frac{p_{CO_2}p_{H_2}^4}{K_3}\right)\Big/\text{DEN}^2 \tag{19}$$

$$\text{DEN} = 1 + K_{CO}p_{CO} + K_{CH_4}p_{CH_4} + K_{H_2}p_{H_2} + \frac{K_{H_2O}p_{H_2O}}{p_{H_2}} \tag{20}$$

where p_{CH_4}, p_{CO}, p_{CO_2} are partial pressures of CH_4, CO and CO_2; k_1, k_2, k_3 are the kinetic coefficients of the three reactions; K_1, K_2, and K_3 are the equilibrium constants of the three reactions; K_{CO}, K_{H_2O}, K_{CH_4} and K_{H_2} are the adsorption constants for CO, H_2O, CH_4, and H_2, respectively, and DEN is a parameter of dimension 1.

The reaction kinetic coefficients k_1, k_2 and k_3 are respectively defined as:

$$k_1 = 9.49\times10^6 \exp\left(-\frac{28\,879}{T}\right) \tag{21}$$

$$k_2 = 4.39\times10^4 \exp\left(-\frac{8074.3}{T}\right) \tag{22}$$

$$k_3 = 2.29\times10^{16} \exp\left(-\frac{29\,336}{T}\right) \tag{23}$$

where the units of k_1, k_2 and k_3 are kmol·kPa$^{0.5}$/(kg·h), kmol·kPa^{-1}/(kg·h), kmol·kPa$^{0.5}$/(kg·h), respectively.

$$K_{CH_4} = 6.65\times10^{-6} \exp\left(\frac{4604.28}{T}\right) \tag{24}$$

$$K_{H_2} = 6.12\times10^{-11} \exp\left(\frac{9971.13}{T}\right) \tag{25}$$

$$K_{H_2O} = 1.77\times10^{3} \exp\left(-\frac{10\,666.35}{T}\right) \tag{26}$$

$$K_{CO} = 8.23\times10^{-7} \exp\left(\frac{8497.8}{T}\right) \tag{27}$$

where the units of K_{CH_4}, K_{H_2}, K_{H_2O} and K_{CO} are kPa^{-1}, kPa^{-1}, –, kPa^{-1}, respectively.

In this study, it is assumed that the chemical reaction during the reforming reaction takes place under chemical equilibrium conditions. This means that the products of the reforming reaction coexist with the reactants at the outlet of the reforming during the reforming process. The equilibrium constants for the three reactions are related to temperature as follows [63]:

$$K_1 = 10\,266.76 \exp\left(-\frac{26\,830}{T} + 30.11\right) \tag{28}$$

$$K_2 = \exp\left(-\frac{4400}{T} - 4.063\right) \tag{29}$$

$$K_3 = K_1 \cdot K_2 \tag{30}$$

where the units of K_1, K_2, and K_3 are kPa^2, –, kPa^2, respectively.

One of the critical parameters for the safe operation of hybrid power systems is the ratio of steam to carbon (S/C). A certain amount of steam is required in the reformer to prevent carbon deposition on the catalyst. In this study, the definition of S/C ratio refers to the ratio of the molar flow rate of steam to the molar flow rate of methane supplied in the reformer [64]. To operate the reformer under safe conditions and prevent carbon deposits in the reformer, a minimum critical value of S/C has been introduced. In the SOFC hybrid system, S/C boundary value depends on the reforming reaction temperature. To ensure the safe operation of the hybrid system, S/C should be controlled above the boundary value. The calculation of S/C is described in the following equation:

$$\text{S/C} = \frac{m_{H_2O,supply}}{m_{CH_4,fuel} + m_{CO_2,fuel}} \tag{31}$$

where $m_{CH_4,fuel}$ is the molar flow of fuel (methane); $m_{H_2O,supply}$ is the molar flow of water; $m_{CO_2,fuel}$ is the molar flow of carbon dioxide.

CH_4 conversion rate X_{CH_4} is described as [65]:

$$X_{CH_4}=\frac{m_{CH_4,in}-m_{CH_4,out}}{m_{CH_4,in}}\times 100\% \quad (32)$$

where $m_{CH_4,in}$ and $m_{CH_4,out}$ are the methane flow at the inlet and outlet of the methane reforming reactor, respectively (mol/s).

The heat loss of the steam reformer can be calculated according to the energy balance equation:

$$m_{14}h_{14}+m_{10}h_{10}=m_8h_8+m_{15}h_{15}+Q_{loss,SR} \quad (33)$$

where $Q_{loss,SR}$ is the heat loss of the methane steam reformer (kJ/s).

3.2.2 Mesh analysis and validation of reformer model

In the symmetrical three-dimensional calculation domain, the geometry of the methane reforming reactor used is more complicated; therefore, the three-dimensional calculation domain is used in the simulation. The catalytic bed in the reformer uses a free quadrilateral mesh, and the insulating jacket and heating tube use a free triangular mesh. Since the catalytic bed near the heating tube has a great influence on hydrogen production by reforming, the boundary layer mesh is used for densification near it. Finally, take the entrance of the catalytic bed and the exit of the heating tube as the source surface to sweep the mesh of the target source surface. The geometry of the methane steam reformer is shown in Fig. 4.

In the steam reformer, the number of mesh near the heating tube and the mesh of the catalytic bed are increased or decreased to verify that the result of the model does not change with the number of mesh. The total number of regular, refined and ultra-refined meshes finally obtained are 45 329, 51 962 and 53 017, respectively. The difference between the ultra-fine mesh and the ultra-refined mesh to produce hydrogen is less than 1.83%. Finally, considering the calculation cost and calculation accuracy, a refined mesh structure was selected as the mesh type of the model. After performing mesh analysis on the reformer model, its performance needs to be verified to determine the reliability of the model.

The purpose of comparing the simulation results with the experimental data [66] is to evaluate the accuracy and performance of the methane steam reformer model proposed in this study, as shown in Table 5. The gas mole fraction at the outlet of the reformer model is compared with the experimental results. The conversion rate and outlet temperature of methane in the reformer are important factors affecting the reforming efficiency, so the conversion rate and outlet temperature are compared with the experimental results. The outlet temperature of the methane steam reformer experiment in the published paper used for the reformer model studied in this paper is 832.25°C, while the temperature at the outlet in the reformer model proposed in this study is 825.48°C. In the model studied in this paper, the temperature at the outlet of the reformer is in good agreement with the temperature at the outlet in the experiment. Table 5 shows the temperature, molar flow rate and gas composition at the outlet of the methane steam reformer model along with literature data used to validate the model. The percentage error between the model's data and the literature data is calculated by dividing the difference between the simulation results obtained in the model and the literature data used for validation (experimental) by the data in the literature. From the results in Table 5, it can be seen that the error between the molar flow at the outlet of the reformer model and the experimental data is negligible. It can be calculated from the table that the simulation results of the reformer model in this paper are consistent with the experimental data, but the error between the model simulation results and the experimental data of the mole fractions of gas components such as H_2, H_2O, and CO is less than 2%, which can be ignored. The gas component with the largest mole fraction error between the simulation results of the reformer model and the experimental data is methane, which is mainly because the methane conversion rate of the reformer model in this paper is 68.19%, while the methane conversion rate of the experimental data is 72%. However, the error of the conversion rate of methane in the reformer model and the experimental data is also less than 5.5%, which can be within the allowable range of error. Therefore, the model used in this study is reasonable and reliable, and can be used for the study of methane steam reforming reaction.

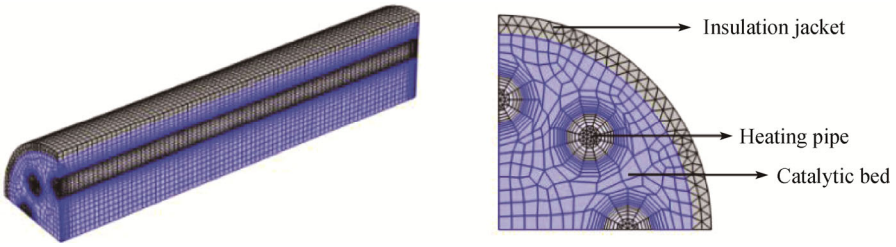

Fig. 4 The mesh geometry of the methane steam reformer

Table 5 Comparison of reformer model results with experimental data

Process-gas mole fraction	Simulation results	Experimental data
H_2 mole fraction/%	45.13	45.82
CH_4 mole fraction/%	5.52	5.05
H_2O mole fraction/%	34.96	35.06
CO_2 mole fraction/%	6.03	5.82
CO mole fraction/%	8.36	8.2
Outlet temperature/°C	825.48	832.35
Methane conversion rate	68.19%	72%
Molar flow at outlet/mol·s^{-1}	8.82	8.97

3.3 Other auxiliary equipment in the system

Other auxiliary equipment in the system mainly includes the afterburner, heat exchanger, air compressor, fuel compressor, water pump and mixer. The specific analysis of auxiliary equipment is as follows.

In a fuel cell, the minimum hydrogen partial pressure is required to protect the anode from oxidation, which means that there is some residual hydrogen and other gases in the anode exhaust gas. The exhaust gas of SOFC contains fuel that is not completely reacted, and the concentration of combustible components is low, and it needs to be burned in the afterburner to improve the fuel utilization rate of the system. These residual gases are combusted with methane in the burner to provide the required heat for the reformer. In the combustor, the residual fuel from the SOFC is burned to heat the fuel gas and water, thereby increasing the temperature of the reaction gas. The efficiency of the combustion process in the afterburner is set to 100% [67]. In the combustor, the residual fuel from the SOFC is completely burned, thereby increasing the temperature of the gas to improve the utilization of system energy. The combustion reaction mechanism is as follows:

$$CH_4 + 2O_2 \rightarrow CO_2 + 2H_2O + Q_{CH_4} \qquad \Delta H = -802 \text{ kJ/mol}$$

$$H_2 + 1/2O_2 \rightarrow H_2O + Q_{H_2} \qquad \Delta H = -241 \text{ kJ/mol}$$

$$CO + 1/2O_2 \rightarrow CO_2 + Q_{CO} \qquad \Delta H = -282 \text{ kJ/mol}$$

Since combustion is an adiabatic process, the enthalpy of the reactant considering the combustion efficiency is equal to the enthalpy of the product. The calculation of the relationship between the enthalpy ΔH of the afterburner and the outlet temperature of the afterburner in the standard state can be calculated by the following equation:

$$m_4 h_4 + m_9 h_9 + m_{19} h_{19} = m_{10} h_{10} + Q_{\text{loss,AB}} \tag{34}$$

where $Q_{\text{loss,AB}}$ is the heat loss of the after combustion chamber (kJ/s).

The system needs a fuel compressor, an air compressor and a water pump to provide the pressure required by the system. In this system, a centrifugal compressor is selected to apply the required pressure to the fuel. The compressor accelerates outward by the impeller to increase the gas pressure. The compressor power is related to the air mole flow rate, which can be obtained by the following formula:

$$W_c = \left(\frac{j}{j-1}\right)\frac{W_{in}u_{in}}{\eta_p}\left[1-\left(\frac{p_{out}}{p_{in}}\right)^{\frac{j-1}{j}}\right] \tag{35}$$

where W_c is the compressor power; u_{in} is the volumetric flow (m^3/s); η_p is the blower efficiency; j is the polytropic coefficient; p_{in} and p_{out} is the pressure at the inlet and outlet of the compressor, respectively. Since the physical properties of the multi-efficiency gas are related to the machine design, the multi-efficiency estimate as a function of the volume flow rate is used [68]:

$$\eta_p = 0.017 \ln u_{in} + 0.7 \tag{36}$$

The variable efficiency is proportional to the volume flow. According to the heat capacity ratio, the multivariable coefficient can be estimated, and the relational equation is estimated as follows:

$$j = \frac{\gamma\eta_p}{\gamma\eta_p - \gamma + 1} \tag{37}$$

where γ is the gas heat capacity ratio.

The water pump used in the system provides steam to the methane reformer. Compared with an air compressor, the volume flow of water in a water pump is very low. Due to the high density of water at ambient temperature and pressure, the molar amount of water and methane required in the system is in a ratio of 1:2.3.

The power consumption of the water pump is:

$$W_{\text{pump}} = \frac{w v_{in}\left(p_{out} - p_{in}\right)}{\eta} \tag{38}$$

where w is the mass flow rate (kg/s); p is the pressure at the outlet and inlet of the pump; v is the specific volume (m^3/kg); η is the efficiency of the pump.

According to the energy balance equation, the heat loss of oxygen compressor, water pump and methane compressor can be obtained:

$$m_1 h_1 = m_2 h_2 + Q_{\text{loss,AC}} \tag{39}$$

$$m_5 h_5 = m_6 h_6 + Q_{\text{loss,WP}} \tag{40}$$

$$m_{11} h_{11} = m_{12} h_{12} + Q_{\text{loss,FC}} \tag{41}$$

where $Q_{\text{loss,AC}}$, $Q_{\text{loss,WP}}$ and $Q_{\text{loss,FC}}$ are the heat loss of air compressor, water pump and methane compressor, respectively (kJ/s).

It can be seen from the system block diagram that there are three heat exchangers in the SOFC-based system for preheating the feed stream of methane and steam and the air supplied to the fuel cell stack. The heat exchanger is a device for the hot fluid to transfer heat

energy to the cold fluid. The heat exchanger used in this system is a counter-flow heat exchanger. The total amount of heat loss in this countercurrent heat exchanger remains constant and independent of load. According to the method used in Ref. [69], the heat exchanger model can be derived:

$$\varepsilon = \frac{C_{\mathrm{hs}}\left(T_{\mathrm{hs,in}} - T_{\mathrm{hs,out}}\right)}{C_{\min}\left(T_{\mathrm{hs,in}} - T_{\mathrm{cs,in}}\right)} = \frac{C_{\mathrm{cs}}\left(T_{\mathrm{cs,out}} - T_{\mathrm{cs,in}}\right)}{C_{\min}\left(T_{\mathrm{hs,in}} - T_{\mathrm{cs,in}}\right)} \quad (42)$$

where the subscripts "cs" and "hs" refer to the cold flow and heat flow in the heat exchanger; C is heat capacity rate (J/K); $C_{\min}$ is the smaller heat capacity ratio between cold flow and hot flow (J/K). Because no chemical reaction occurs in the heat exchanger, the fluid molar flow rate and fuel mole fraction at the inlet and outlet of each node of the heat exchanger are the same. The heat exchanger model is described according to the energy balance equation, so the latent heat of water turning into steam must be considered in the modeling process.

As shown in Fig.1, there are three preheaters in the SOFC integrated system, which are used to preheat methane and steam for the steam reforming reaction, and to supply air to the SOFC. The heat balance equation of these heat exchangers can be determined:

$$m_{12}h_{12} + m_{15}h_{15} = m_{16}h_{16} + m_{13}h_{13} + Q_{\mathrm{loss,HEX1}} \quad (43)$$

$$m_{6}h_{6} + m_{16}h_{16} = m_{7}h_{7} + m_{17}h_{17} + Q_{\mathrm{loss,HEX2}} \quad (44)$$

$$m_{2}h_{2} + m_{17}h_{17} = m_{3}h_{3} + m_{18}h_{18} + Q_{\mathrm{loss,HEX3}} \quad (45)$$

where $Q_{\mathrm{loss,\ HEX1}}$ $Q_{\mathrm{loss,\ HEX2}}$ and $Q_{\mathrm{loss,\ HEX3}}$ are the heat loss of heat exchangers 1, 2 and 3, respectively (kJ/s).

The test results of the heat exchanger in the experiment show that stable operation at high temperatures can be achieved. Considering that the heat exchanger operates under high temperature conditions, a welded plate heat exchanger is selected. Under various gas flow, pressure and temperature conditions, the heat energy loss of the heat exchanger is 3.2%, and the efficiency is 80%–89%. Therefore, based on the above results, the heat exchanger can be used in the system.

For SOFC-based systems, water vapor is mixed with fresh fuel feed in a mixer and then passed into a methane steam reformer. The heat loss of the mixer can be calculated according to the energy balance of the mixer as:

$$m_{7}h_{7} + m_{13}h_{13} = m_{14}h_{14} + Q_{\mathrm{loss,M}} \quad (46)$$

where $Q_{\mathrm{loss,M}}$ is the heat loss of the mixer (kJ/s).

The sum of heat losses from auxiliary equipment such as the air compressor, fuel compressor, water pump, afterburner, three heat exchangers and mixers is calculated as follows:

$$\begin{aligned} Q_{\mathrm{loss,a}} = {} & Q_{\mathrm{loss,HEX1}} + Q_{\mathrm{loss,HEX2}} + Q_{\mathrm{loss,HEX3}} + Q_{\mathrm{loss,M}} \\ & + Q_{\mathrm{loss,FC}} + Q_{\mathrm{loss,AC}} + Q_{\mathrm{loss,WP}} + Q_{\mathrm{loss,AB}} \end{aligned} \quad (47)$$

4. System Performance Evaluation Criteria

The total system efficiency is defined as the ratio of the AC power output by the stack to the low heating value of the fuel entering the system. The efficiency of the SOFC combined system:

$$\eta_{\mathrm{sys,CH_4}} = \frac{W_{\mathrm{SOFC}}}{m_{\mathrm{CH_4,in}}\mathrm{LHV}_{\mathrm{CH_4}}} \quad (48)$$

The net efficiency of the system is defined as the ratio of the net power output from the stack (the output power of the stack minus the parasitic power) and the low calorific value of the efficiency entering the system. Parasitic power is defined as the additional power consumption of auxiliary equipment (compressors and water pumps) in the system, mainly compressors, thereby reducing the net power generation efficiency of the system. The net efficiency of the SOFC combined system:

$$\eta_{\mathrm{sys,CH_4}} = \frac{W_{\mathrm{net}}}{\left(m_{\mathrm{CH_4,in}}\mathrm{LHV}_{\mathrm{CH_4}}\right)_{\mathrm{MSR}} + \left(m_{\mathrm{CH_4,in}}\mathrm{LHV}_{\mathrm{CH_4}}\right)_{\mathrm{AB}}} \quad (49)$$

The net power of the SOFC combined system is as follows:

$$W_{\mathrm{net}} = W_{\mathrm{SOFC}} - W_{\mathrm{FC}} - W_{\mathrm{AC}} - Q_{\mathrm{loss,total}} \quad (50)$$

In the new integrated system, the fuel supplied to this new system includes the fuel energy supplied to the steam reformer and the afterburner, and part of the electrical energy generated by the SOFC is used for the operation of the methane compressor and the air compressor. Through the temperature, fuel cell output power, flow rate and pressure data obtained through the simulation, the enthalpy value of each node is then calculated. The calculated enthalpy value can be used to calculate the heat loss of SOFC, steam reformer, afterburner, heat exchanger and water pump. For the energy balance equation of the entire system, the heat energy loss of each component can be obtained:

$$\begin{aligned} & \left(m_{\mathrm{in}}\mathrm{LHV}_{\mathrm{CH_4}}\right)_{\mathrm{MSR}} + \left(m_{\mathrm{in}}\mathrm{LHV}_{\mathrm{CH_4}}\right)_{\mathrm{AB}} + \sum_{k}^{N} W_{\mathrm{cp}} \\ & = W_{\mathrm{SOFC}} + Q_{\mathrm{loss,total}} + Q_{\mathrm{fuel}} \end{aligned} \quad (51)$$

where m_{in}, LHV, W_{cp}, W_{SOFC}, $Q_{\mathrm{loss,total}}$ and Q_{fuel} are the flow of methane into the steam reformer and afterburner, the low heating value of the fuel, the output power of SOFC used for methane compressor and air compressor power, the output power of SOFC, the loss of heat energy in the entire system and the chemical energy of unreacted fuel in the system, respectively.

The energy loss of each component is calculated according to the energy balance equation of each component. The total heat loss of the SOFC and reformer hydrogen production integrated system is the sum of the individual heat losses of the SOFC, reformer, afterburner and other components. The total heat loss is specifically:

$$Q_{\text{loss,total}} = \sum_{i=1}^{k} Q_{\text{loss},k} = Q_{\text{loss,SOFC}} + Q_{\text{loss,SR}} + Q_{\text{loss,a}} \quad (52)$$

where k is the heat loss from each component in the integrated system.

For the SOFC combined system, the numerical solution of the SOFC system model is quite complicated due to the interaction between SOFC and other subsystems. The detailed design parameters of the SOFC combined system are shown in Table 6.

In this paper, an integrated system of SOFC and external reforming for hydrogen production is proposed. Before any practical application of the system, a comprehensive theoretical analysis must be carried out to evaluate the performance of the system combination. Therefore, based on the mathematical model, the proposed system is simulated under steady-state conditions. Use COMSOL Multiphysics 5.6 and Aspen Plus simulation tools to simulate the SOFC system of methane steam reforming to hydrogen. Carrying out energy balance analysis helps to ensure the stability of the energy system with SOFC at its center. At the same time, improving system performance is the center of the SOFC energy system for methane steam reforming to produce hydrogen. In this study, based on the laws of thermodynamics, the analysis and calculation of the SOFC system for hydrogen production by methane steam reforming can better study the performance of the system. In the external methane steam reforming SOFC system, the operating temperature and pressure of the SOFC are

Table 6 Design parameters of SOFC integrated system

SOFC operating parameters		
Cell operating temperature	800	°C
Air composition	21% O_2, 79% N_2	–
Fuel cell active area	0.1	m^2
Cell operating pressure	101.56	kPa
DC/AC inverter efficiency	98	%
Ambient temperature	25	°C
Ambient pressure	101.32	kPa
SOFC pressure drop	2	%
Number of cells	20 000	–
Universal gas constant	8.314	J/(mol·K)
Methane steam reforming operating parameters		
Operating temperature	1041.9	°C
S/C	2.5	–
Ambient pressure	101.32	kPa
Pressure loss	2	%
Auxiliary equipment parameters		
Afterburner efficiency	100	%
Fuel compressor isentropic efficiency	98	%
Air compressor isentropic efficiency	85	%
Pump isentropic efficiency	90	%
Afterburner pressure drop	3	%
Pressure drop of heat exchanger	2	%
Fuel compressor pressure ratio	1.3	–
Effectiveness of heat exchanger	78	%
Air compressor pressure ratio	1.32	–
Compressor pressure loss	1	%

Table 7 Parameters of each node of the power system are based on SOFC

Node	T/°C	p/kPa	m/mol·s^{-1}	Mole fraction/%					
				CH_4	H_2	CO_2	H_2O	O_2	N_2
1	25.00	101.33	0.27	0	0	0	0	21	79
2	44.02	121.59	0.27	0	0	0	0	21	79
3	761.31	122.71	0.27	0	0	0	0	21	79
4	800.00	120.52	0.263	0	0	0	0	18.63	81.37
5	25.00	101.33	0.0018	0	0	0	100	0	0
6	25.00	121.59	0.0018	0	0	0	100	0	0
7	746.31	121.59	0.0018	0	0	0	100	0	0
8	771.80	123.08	0.0027	14.82	59.26	11.11	14.81	0	0
9	800.00	120.68	0.0097	4.12	9.28	3.09	83.51	0	0
10	1041.9	131.7	0.2745	0	0.33	0.29	10.46	10.97	77.95
11	25.00	101.33	0.0009	100	0	0	0	0	0
12	40.32	121.59	0.0009	100	0	0	0	0	0
13	753.11	121.59	0.0009	100	0	0	0	0	0
14	749.31	122.59	0.0027	33.33	0	0	66.67	0	0
15	759.85	103.33	0.2745	0	0.33	0.29	10.46	10.97	77.95
16	758.11	226.07	0.2745	0	0.33	0.29	10.46	10.97	77.95
17	751.31	226.07	0.2745	0	0.33	0.29	10.46	10.97	77.95
18	102.73	102.06	0.2745	0	0.33	0.29	10.46	10.97	77.95
19	25.00	101.33	0.0018	100	0	0	0	0	0

800°C and 102 kPa, respectively. The steam to carbon ratio of the methane steam reformer is fixed at 2.5. The performance model of each subsystem in the SOFC system of the methane steam reformer is summarized. Table 7 lists the thermodynamic parameters of each node of the energy system based on SOFC as the center. Under given operating conditions, the power generation efficiency of the external methane reforming hydrogen production SOFC system can reach 52.52%, which can be further improved through parameter optimization.

5. System Energy Balance Analysis

Energy in the system is considered as a property of the object, which can make the object work by transforming it into various forms of energy. Therefore, energy analysis helps to understand the energy in the system that changes with the environmental change. The energy loss of each component can be calculated from the energy balance equation of each subsystem in the integrated system. Table 8 lists the energy analysis results of this study based on previous assumptions. The SOFC system for hydrogen production by steam reforming of methane analyzes the energy balance of the system under the conditions of an operating temperature of 800°C and steam to carbon ratio of 2.5.

Table 8 Energy analysis results of SOFC integrated system

Item	Value/W	Ratio/%
Energy input		
Methane as fuel	1771.83	100
Heat loss		
SOFC	240.73	13.59
Methane steam reformer	123.49	6.97
After burner	70.45	3.98
Air compressor	61.38	3.46
Fuel compressor	38.89	2.2
Water pump	43.27	2.44
Heat exchanger 1	23.61	1.33
Heat exchanger 2	51.87	2.93
Heat exchanger 3	64.36	3.63
Mixer	22.61	1.28
Exhaust gas loss	100.6	5.68
Total energy loss	823.45	47.48
Energy output		
Output power	930.57	
Sum of energy	1771.83	100
Net efficiency		52.52

In Fig. 1, stream 18 represents waste heat loss, that is, unused waste heat energy in the SOFC system for steam reforming of methane to produce hydrogen. In the SOFC distributed energy system for methane steam reforming and hydrogen production, the SOFC subsystem, reforming hydrogen production subsystem, and waste heat utilization system are introduced. The full use of the medium and low temperature heat source carried by the exhaust gas in the SOFC subsystem can improve the energy utilization rate and power generation efficiency of the system. Table 9 provides the power efficiency of the system in the energy balance of the SOFC system for methane steam reforming to hydrogen is 52.52%. It is equivalent to the net output power and efficiency of the external reforming hydrogen generation system in the existing reference and the system in this study. At the same time, the methane steam reforming hydrogen production SOFC system makes full use of heat energy and has advantages in energy efficiency. Therefore, it can be seen from the energy analysis results that the system in this study saves energy and has higher fuel utilization during the production process.

In the energy system with SOFC as the center, the energy flow starts from the reformer and the afterburner, and the two subsystems generate 1771.83 W, which is recognized as 100%. In the energy loss analysis, the top three energy losses are the heat energy carried by the SOFC, the methane steam reformer and the exhaust gas in the system, and the corresponding proportions are 13.59%, 6.97% and 5.67%, respectively. The fuel cell energy loss of 240.73 W is mainly because the H_2 used in the SOFC using the reforming system comes from the reforming reaction of the fuel, and the remaining heat energy is used to heat the fuel and air in the system. From the energy analysis, it can be seen that the maximum energy loss of SOFC is 240.73 W, which is the irreversible electrochemical reaction in SOFC and the energy loss during DC/AC conversion. The SOFC converts the chemical energy of hydrogen into electrical energy and waste heat, and the waste heat in the fuel cell causes a large energy loss. Therefore, the main way to improve the performance of the energy system is to reduce the energy loss in the fuel cell. Increasing the operating temperature and operating pressure of the fuel cell can promote the progress of the electrochemical reaction and reduce the energy loss of the SOFC. In addition, reducing the heat loss in the fuel cell and good heat insulation measures can be an important measure to reduce the energy loss in the SOFC. The reforming reaction in the methane steam reformer is an endothermic reaction, which can absorb the waste heat of the fuel cell, thereby converting the waste heat into the chemical energy of hydrogen, which will make the methane reformer produce less energy loss.

From the energy analysis table, the energy loss of other subsystems of the SOFC energy system for

methane steam reforming to hydrogen can be drawn: the energy loss of the afterburner is 70.45W, which is mainly the irreversible combustion loss, which can be selected by the appropriate air and fuel flow. The total energy loss of the three heat exchangers in the system is 139.84 W, which accounts for 7.89% of the input energy of the system. By selecting the appropriate heat exchange temperature difference, the energy loss of the heat exchange part can be reduced. The energy taken away by the exhaust gas in the system is 100.4 W, which accounts for 5.67% of the system output energy. To make full use of the waste heat of the exhaust gas, it is possible to use the exhaust gas to a lower temperature while ensuring that the temperature of the exhaust gas is higher than the ambient temperature, so as to reduce the energy taken away by the exhaust gas. Through energy analysis, the weak links of system energy utilization can be found, and system performance can be optimized by improving SOFC performance, optimizing heat exchanger layout, and minimizing heat exchange temperature differences to improve system performance.

6. Performance Features and Discussion

In the entire system, key parameters such as the operating temperature of the SOFC, the operating temperature of the reformer, and the flow of fuel have a great impact on the performance of the system. Therefore, it is necessary to perform parameter analysis in the evaluation index of system performance to evaluate the change of each important parameter to the output power and efficiency of the system. In this system, the researched parameters mainly include SOFC operating temperature, steam reformer operating temperature and reformer steam-to-carbon ratio on the performance of the SOFC-based energy integration system. In the analysis of an integrated system with parameters as the center of SOFC, one parameter changes, while the others remain unchanged.

6.1 Influence of reformer temperature on system performance

In the reformer, methane steam reforming to produce hydrogen is a highly endothermic reaction process. The operating temperature of the reformer is a very important design and operating parameter, which is directly related to the degree of equilibrium conversion and the composition of the final reaction product. In the hydrogen production reaction of methane steam reforming, temperature affects the distribution of components in the reformer, the generation of H_2 and the reaction rate of various substances, and even the service life of the reformer. Therefore, the evaluation of reformer performance at different temperatures is of great significance for practical applications. To analyze the influence of the operating temperature of the reformer on the performance of the system, the operating temperature of the SOFC is fixed at 800°C; the ratio of steam to carbon is 2.5, and the pressure is 131.72 kPa. The influence of reformer operating temperature on fuel cell performance is shown in Fig. 5. The influence of the working temperature of the reformer on the net power and efficiency of the methane steam reforming hydrogen production and SOFC system is shown in Fig. 6.

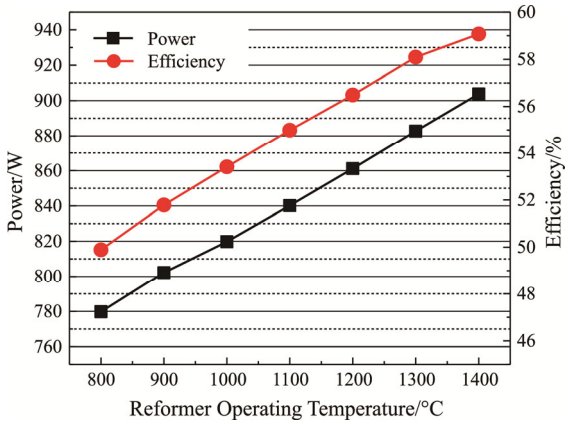

Fig. 5 Influence of reformer operating temperature on fuel cell performance

It can be seen from Fig. 5 that as the operating temperature of the methane steam reformer increases, the power of the fuel cell increases from 779.82 W to a maximum power of 903.81 W. The efficiency increased from the minimum efficiency of 49.89% to 59.07%, an increase of 9.18 percentage points. Because the methane steam reforming reaction is a strongly endothermic reaction, raising the temperature is beneficial to the progress of the reaction. As the operating temperature in the reformer increases, the conversion rate of methane increases, and the amount of hydrogen produced in the reformer gradually increases. When the reforming temperature is lower than 900°C, the methane conversion rate is lower than 75%, and the temperature of the exhaust gas of the reformer is also low. After the unreacted methane in the reformer enters the fuel cell stack, it will continue to react under the catalysis of nickel in the catalyst layer of the anode of the fuel cell stack. The reaction of methane and water vapor needs to absorb a lot of heat, while the heat generated by the fuel cell stack is very small, which causes the internal temperature of the stack to drop rapidly and the ohmic polarization is more serious, making the efficiency of the electric fuel cell lower than 51.79%. The operating temperature of the reformer is 900°C, 1000°C, 1100°C, 1200°C and 1300°C, and corresponding to the fuel cell efficiency of 51.79%, 53.41%, 54.99%, 56.49% and

58.09%, respectively. When the reforming temperature is greater than 900°C, the methane steam reforming reaction speeds up in the positive direction, and the methane conversion rate is greater than 83%. However, there is less unconverted methane in the reformer, and less heat is absorbed by the reaction of methane and steam after entering the fuel cell stack. At the same time, the increase in hydrogen production increases the partial pressure of hydrogen in the fuel gas, so the efficiency of the fuel cell stack increases.

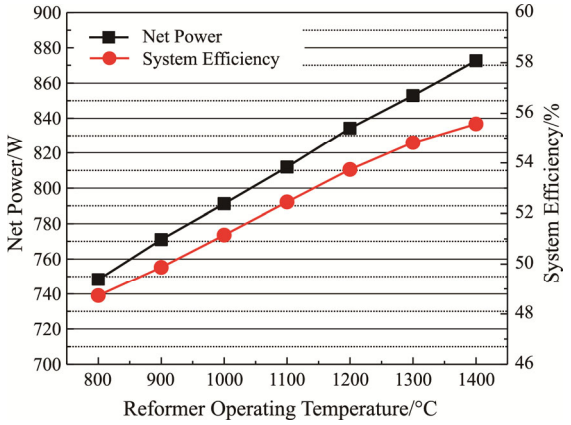

Fig. 6 Influence of the operating temperature of the reformer on the net power and efficiency of the system

It can be seen from Fig. 6 that as the operating temperature of the methane steam reformer runs from 800°C to 1400°C, the net power of the SOFC and methane steam reformer system increases from 748.28 W to 872.55 W, and the efficiency increases from 48.73% to 55.57%. Because as the reforming temperature of the reformer increases, the temperature of the reformed gas entering the fuel cell stack increases, and the temperature difference between the reformed gas and the fuel cell stack is small, and heat balance can be achieved. It avoids the performance degradation caused by the entry of low-temperature reformed gas that reduces the local temperature in the fuel cell stack. Moreover, when the reformer is operating under low temperature conditions, the incompletely reacted methane enters the fuel cell stack and reforms with water vapor again. The fuel cell stack generates less heat, and the reforming reaction inside the fuel cell absorbs heat. Therefore, the increase of the reforming temperature is beneficial to improving the performance of the stack.

As the operating temperature of the reformer increased from 800°C to 1000°C, the net power and efficiency of SOFC and methane steam reforming hydrogen production systems increased by 124.27 W and 6.84%, respectively. Increasing the operating temperature of the reformer is beneficial to increase the utilization rate of the catalyst in the reformer, and at the same time increases the equilibrium constant and reaction rate of the reforming hydrogen production reaction, and promotes the conversion of methane to produce more hydrogen, which improves the efficiency of the system. Because the methane steam reforming reaction is an endothermic reaction, the activity of the catalyst in the reformer is greatly affected by temperature. The catalytic activity of the catalyst gradually becomes better when the reformer runs at high temperatures, which improves the efficiency of the reforming reaction, and the reforming reaction produces more hydrogen, which is supplied to the SOFC anode to react with oxygen to generate more electricity. The methane steam reforming reaction is a strongly endothermic reaction, while the water gas shift reaction is an exothermic reaction. These two reactions exist in the reformer reaction system at the same time, and the effects of temperature on the two reactions are different. Therefore, increasing the operating temperature of the reformer is conducive to the conversion of CH_4 to hydrogen but not to the conversion of carbon monoxide. As the temperature increases, the CH_4 conversion rate increases significantly, and the exothermic water-gas shift reaction is inhibited because the increase in temperature at this time promotes the steam reforming reaction more than it inhibits the water-gas shift reaction. Therefore, the content of H_2 in the product still increases with increasing temperature. The operating temperature of the reformer is 900°C, 1000°C, 1100°C, 1200°C and 1300°C; the power generation efficiency of the corresponding system is 49.87%, 51.15%, 52.45%, 53.74% and 54.81%, respectively. When the operating temperature of the reformer gradually increases from 800°C to 1400°C, the CH_4 conversion rate increases by 25%; the H_2 yield increases correspondingly, and the hydrogen volume fraction in the reformed gas component increases. Therefore, the efficiency and output of the SOFC system for hydrogen production by methane steam reforming increase with the increase of the reforming temperature.

The methane steam reforming reaction is an endothermic reaction, and the increase of the reaction temperature is conducive to the improvement of the methane conversion rate. When the operating temperature of the reformer rises, the methane content in the reformed gas will decrease when equilibrium is reached, and the effective gas concentration of H_2 will increase accordingly. The conversion rate of methane depends on the temperature. When the temperature increases from 800°C to 1400°C, the methane conversion rate increases from about 63.6% to 89.6%, with an increase of nearly 26%. The operating temperature of the reformer is 1400°C, and the efficiency of the SOFC system for methane steam reforming to hydrogen is 55.57%, but an appropriate operating temperature should be selected in consideration of system performance.

Compared with the steam to carbon ratio, the temperature has a greater impact on the performance of the SOFC system, but the reaction temperature is limited by the high temperature strength and service life of the reformer material. In theory, increasing the operating temperature of the reformer is beneficial to production, but in actual production, the selection of the reformer temperature should consider the requirements of the production process, the characteristics of the catalyst and the performance of the heating tube material.

6.2 Effect of steam to carbon ratio on system performance

In the process of studying the influence of steam-to-carbon ratio on the performance of SOFC and external reforming hydrogen production system, the operating temperature of the fuel cell and reformer are 800°C and 905°C, respectively. The fuel utilization rate of the fuel cell stack remains 0.85. The steam to carbon ratio is adjusted by changing the concentration of methane and water entering the reformer. The steam-to-carbon ratio directly affects the reformer outlet and also the fuel composition at the SOFC anode inlet, which in turn affects the electrochemical performance of the SOFC. In addition, a reasonable steam-to-carbon ratio also plays a role in preventing carbon deposits in the reforming reaction and ensuring the safe operation of the reformer. Changes in the steam-to-carbon ratio in SOFC and external reforming hydrogen production systems will cause the changes in the concentration of fuel gas components entering the fuel cell, which will affect the performance of the entire system. The performance of the SOFC and reforming hydrogen production system when the steam-to-carbon ratio changes between 1 and 3 is shown in Fig. 7.

It can be seen from Fig. 7 that as the ratio of steam to carbon increases, the output power of the fuel cell drops from 881.65 W to 845.54 W, and the corresponding

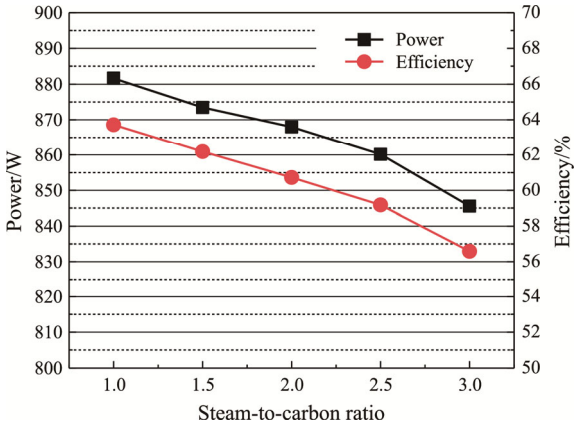

Fig. 7 Effect of steam to carbon ratio on the performance of the SOFC

efficiency also drops from 63.72% to 56.59%. Because as the ratio of steam to carbon increases, the amount of hydrogen produced by methane steam reforming to produce hydrogen increases rapidly, and the current density generated by the electrochemical reaction between the feed fuel cell and air increases. However, the water vapor and carbon dioxide produced by the increase in the steam-to-carbon ratio dilute the hydrogen in the anode electrode of the SOFC. The higher water pressure and lower hydrogen partial pressure in the SOFC stack reduce the theoretical open-circuit voltage of the fuel cell. In addition, the hydrogen partial pressure is a function of the voltage loss of the fuel cell. Due to the dilution effect of water vapor and carbon dioxide, an increase in the steam-to-carbon ratio will cause the anode to produce greater concentration polarization and activation polarization. The steam to carbon ratio of the SOFC and methane steam reformer is increased from 1 to 3, and the power of the fuel cell decreases from the maximum output power of 881.65 W to the minimum output power of 845.54 W. The efficiency dropped from the maximum efficiency of 63.72% to 56.59%, and the efficiency dropped by 7.13 percentage points. The increase of the steam-to-carbon ratio increases the total volume flow of the reformed gas, which can take away the reaction products of the anode in time, so that the fuel can be replenished in time, thus increasing the electrochemical reaction rate and output power. The ratio of steam to carbon increases from 1 to 3 with an interval of 0.5, and the efficiencies of SOFC are 63.72%, 62.18%, 60.72%, 59.18% and 56.59%, respectively. As the steam-to-carbon ratio increases, the heat absorbed by the methane steam reforming reaction will increase; the heat released by the water-gas shift reaction will increase; the cold cut effect of water vapor on the fuel cell will increase; the combined effect will lead to a decrease in the operating temperature of the fuel cell. In this case, the ohmic polarization and electrode polarization resistance in the fuel cell increase. The internal voltage loss caused by the polarization resistance of the fuel cell increases, so that the voltage of the fuel cell decreases; the output power of the fuel cell decreases and the power generation efficiency of the fuel cell also decreases. The effect of steam to carbon ratio on the net power and efficiency of methane steam reforming hydrogen production and SOFC systems is shown in Fig. 8.

It can be seen from Fig. 8 that as the steam-to-carbon ratio increases from 1 to 3, the net output power of the system decreases from 852.53 W to 809.76 W, and the power generation efficiency decreases from 61.75% to 48.19%. Because as the ratio of steam-to-carbon increases, the output power of the fuel cell decreases, and the steam reforming reaction absorbs heat. The power of the air compressor has an impact on the net power and

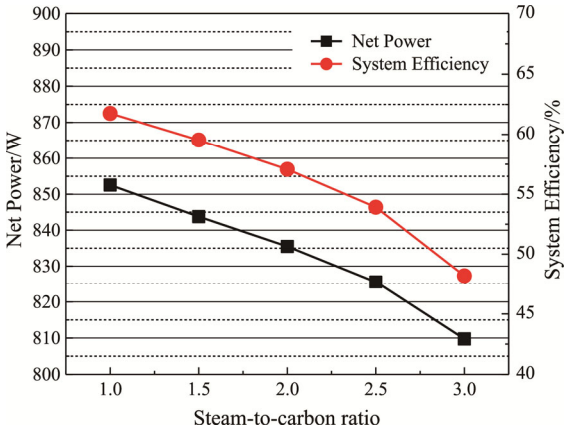

Fig. 8 Effect of steam-carbon ratio on integrated system performance

efficiency of the system, and it needs to be adjusted by the airflow rate to maintain the operating temperature of the SOFC at the required temperature of 800°C. Under the condition that the operating temperature of SOFC remains the same, increasing the ratio of steam to carbon will cause the fuel cell to lose a lot of heat during the electrochemical process, and it is necessary to increase the air flow rate in the system to keep the fuel cell operating temperature stable. In addition, the anode exhaust gas concentration of the fuel cell is low, which reduces the amount of heat generated in the afterburner. Therefore, the increase in air flow in the air compressor increases the power consumption, which reduces the efficiency of the SOFC system for hydrogen production from methane steam reforming from the maximum value of 61.75% to the minimum value.

The steam-to-carbon ratio of the SOFC and methane steam reforming hydrogen production unit increases from 1 to 3, the net power of the system drops from 852.53 W to 809.76 W, and the efficiency drops from the maximum efficiency of 61.75% by 13.6 percentage points to the minimum efficiency. The steam-to-carbon ratio increases from 1 to 3 at an interval of 0.5, and the efficiencies of the external reforming hydrogen production and SOFC integrated system are 61.75%, 59.53%, 57.07%, 53.91% and 48.19%, respectively. Because the steam entering the SOFC and methane steam reforming hydrogen production system is liquid water at room temperature, it must be heated to the steam state before the steam reformer reacts, which requires a large amount of phase change heat. In the system, it is difficult to recover the latent heat of water vapor in the product of hydrogen reforming by the reformer. Therefore, the higher the steam-to-carbon ratio, the lower the efficiency of the SOFC and methane steam reformer system when the latent heat of vaporization taken away by the steam in the reformer is 10.46% or more.

From the calculation results, it can be seen that reducing the steam-to-carbon ratio can improve the power generation efficiency and output of the SOFC and methane steam reforming hydrogen production system, but the steam-to-carbon ratio is too low to easily cause carbon deposits in the reformer. In addition, an increase in the steam-to-carbon ratio can increase the reaction rate and inhibit the carbon deposition reaction. However, the level of steam-to-carbon ratio is directly related to energy consumption, so choosing an appropriate steam-to-carbon ratio is a very important design and operating parameter in the methane steam reforming process.

6.3 Influence of SOFC operating temperature on system performance

In the SOFC integrated system for steam reforming of methane to hydrogen, the operating parameters of the SOFC affect the output power and efficiency of the entire system. Therefore, it is necessary to study the key operating parameters of SOFC. The operating temperature of SOFC is an important operating parameter that affects fuel cell performance. The drastic changes in the internal temperature of the fuel cell will also cause a greater temperature gradient, which will cause problems such as SOFC delamination and fracture, and cause irreversible performance loss to the fuels cell. The temperature change is related to the polarization loss inside the fuel cell, which in turn affects the power generation performance of the SOFC. In this paper, a simulation study is carried out through the model of the power generation system. When the operating temperature changes in the range of 600°C to 1000°C, the output performance and efficiency of the SOFC and methane steam reforming hydrogen production system are affected. The methane steam reformer has a temperature of 905°C, a steam-to-carbon ratio of 2.5, and pressure of 1.3 kPa. The influence of SOFC operating parameters on the output power and efficiency of the fuel cell is shown in Fig. 9. The influence of the operating temperature of SOFC on the performance of the power generation system with SOFC as the center is shown in Fig. 10.

It can be seen from Fig. 9 that as the SOFC operating temperature increases from 600°C to 1000°C, the output power of the fuel cell increases from 883.34 W to 937.58 W, and the efficiency increases from 49.38% to 61.59%. Because the operating temperature of SOFC is directly related to the loss of concentration polarization and activation polarization, and ohmic polarization is inversely proportional to the operating temperature of SOFC. Therefore, as the operating temperature of the fuel cell increases, the activation polarization and concentration polarization become higher. Compared with the ohmic loss, the concentration polarization and activation polarization are very small. On the other hand,

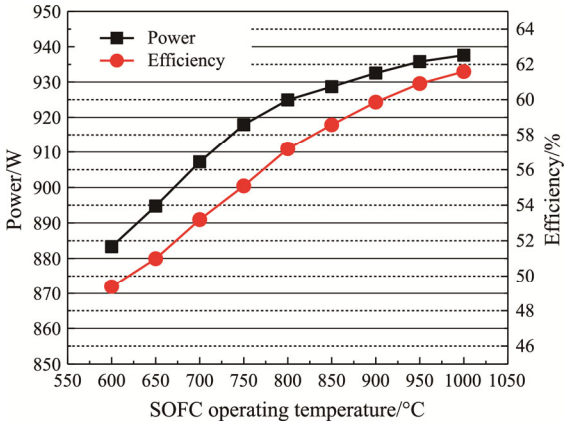

Fig. 9 The influence of SOFC operating temperature on fuel cell performance

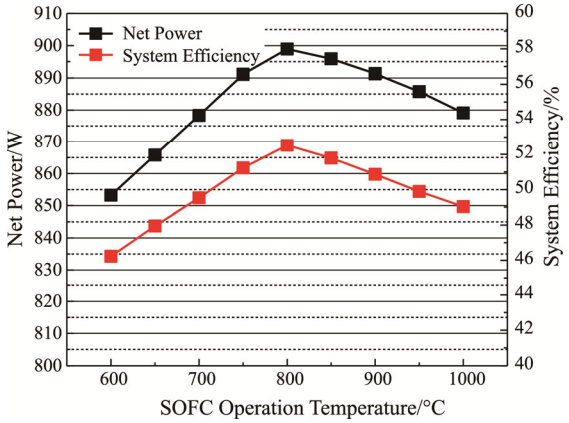

Fig. 10 The influence of the operating temperature of the SOFC on the net power and efficiency of the integrated system

based on the Nernst voltage equation, increasing the operating temperature of the SOFC will increase the Gibbs free energy and decrease the Nernst voltage. Therefore, increasing the operating temperature of the SOFC increases the open circuit voltage and lowers the ohmic loss, which can improve the output power and efficiency of the fuel cell. According to the different SOFC electrolytes, the higher the SOFC temperature, the higher the conductivity of the SOFC, which depends on the characteristics of the ceramic, thereby reducing the ohmic loss. The operating temperature of SOFC is 700°C, 750°C, 800°C, 850°C, 900°C and 950°C, and the corresponding efficiencies are 53.19%, 55.08%, 57.18%, 58.57%, 59.86% and 61.59%, respectively. The efficiency of a fuel cell operating SOFC under low temperature conditions is worse, because the ohmic resistance of the electrolyte is greater at low temperatures. Therefore, increasing the operating temperature of the fuel cell can increase the output power and efficiency of the fuel cell. However, considering that when the temperature of the SOFC stack is too high, the electrodes will be sintered, and chemical reactions will occur between the electrodes and the electrolyte components, which will cause problems such as battery sealing and short life.

It can be seen from Fig. 10 that as the SOFC operating temperature increases from 600°C to 1000°C, the net power and efficiency of the SOFC system for hydrogen production from the methane steam reformer first increase to the maximum net power and maximum efficiency and then decrease. As the operating temperature of the SOFC increases to 800°C, the maximum net power and maximum efficiency of the SOFC system for hydrogen production from the methane steam reformer are 899.93 W and 52.52%, respectively. Because the operating temperature of SOFC is between 600°C and 800°C, the energy loss of methane steam reforming accounts for 9.94%, 9.04% and 7.25% of the total energy input, respectively. The average energy loss of SOFC energy in this temperature range accounts for 12.01% of the total input energy. Among the SOFC operating temperatures studied, the SOFC operating temperature is 800°C, and the energy loss carried by the exhaust gas of the system is the smallest 100.4 W, which accounts for 5.67% of the total energy input. When the SOFC operating temperature is 800°C, the energy loss of the methane steam reformer is also the smallest 123.49 W, accounting for 6.97% of the total energy input. The temperature of the entire system used for methane steam reforming to produce hydrogen increases; the waste heat available for reforming reactions increases, and the hydrogen fed to the SOFC increases, which increases the output power of the fuel cell and the efficiency of the system. The operating temperature of the SOFC is related to the equilibrium voltage, and the actual voltage increases as the operating temperature of the SOFC increases. The increasing trend of Nernst voltage is greater than the sum of the increasing trends of activation polarization and concentration polarization. In addition, as the operating temperature of the SOFC increases, the power generation of the SOFC system used for methane steam reforming to produce hydrogen increases, and gradually reaches a maximum net power of 899.93 W and a maximum efficiency of 52.52%.

The operating temperature of SOFC is increased from 600°C to 800°C; the net power of the system is increased by 45.71 W, and the efficiency is increased by 6.54%. However, the operating temperature of SOFC increased from 800°C to 1000°C, and the net power and efficiency of the system decreased from the maximum value to 879.08 W and 49.03%, respectively. According to Faraday's equation, when the current density remains the same, the amount of fuel involved in the electrochemical reaction remains the same. As the SOFC operating temperature rises to 800°C, the reaction rate of the fuel

cell increases; the oxygen utilization rate increases, and the air volume at the cathode inlet of the system decrease, and the power is required by the air compressor decreases from 32.73 W to 25.08 W. However, the operating temperature of SOFC is higher than 800°C, and the net power and efficiency of the SOFC system for methane steam reforming to produce hydrogen gradually decreases from the maximum. When the reaction rate reaches a certain value, the operating temperature of the SOFC increases, and more air is needed at the cathode inlet of the fuel cell to take away the excess heat generated by the temperature increase, which increases the power required by the air compressor from 25.08 W to 40.83 W. When the operating temperature of the SOFC is higher than 800°C, the increase in the output power of the fuel cell slows down, while the power required by the air compressor increases, and the energy loss carried in the exhaust gas of the system increases from the minimum value of 800°C to 158.09 W. Therefore, when the operating temperature of the SOFC reaches 800°C, the net power and efficiency of the system will decrease from the maximum value. The high operating temperature of the SOFC will increase the temperature of the fuel gas at the outlet of the fuel cell, which will also increase the temperature of the afterburner. Therefore, more oxygen is needed from the cathode of the fuel cell to control the temperature of the afterburner, so that the SOFC operating temperature increases to 1000°C and the air compressor consumes more electric energy. The operating temperature of the SOFC increased from 600°C to 800°C, and the electrical energy required by the air compressor increased by 28.15 W on average. The operating temperature of the SOFC increased from 800°C to 1000°C, and the electrical energy required by the air compressor increased by 49.66 W on average. Therefore, the operating temperature of SOFC is less than 800°C; the net power and efficiency of the SOFC system for methane steam reforming to produce hydrogen gradually increase, and the operating temperature of SOFC is greater than 800°C, and the net power and efficiency of the system decrease.

7. Conclusions

In this study, a model of SOFC combined power generation system using methane as a fuel for steam reforming to produce hydrogen was established. The SOFC reactor and reformer modules are simulated by the multi-physics simulation software COMSOL Multiphysics 5.6, and the simulation results are verified with the experimental results. The performance under design conditions is analyzed. SOFC operating temperature, water vapor to carbon ratio and reformer temperature are three key operating parameters, and their influences on system performance have been studied. At the same time, the energy analysis of the system is carried out according to the law of thermodynamics. The main conclusions are as follows:

The SOFC combined power generation system that uses the external reforming of methane fuel to produce hydrogen can achieve a power generation efficiency of 52.52%, which can be further improved through parameter optimization under given conditions to increase the efficiency and output power of the system. When the ratio of steam to carbon and the operating temperature of the reformer are 2 and 1200°C, the net output power and efficiency of the system will be 835.47 W, 861.09 W and 57.07%, 56.49%, respectively, which affects the power and efficiency of the output SOFC subsystem. However, considering the safety and life of the system, an appropriate steam-to-carbon ratio and operating temperature of the reformer should be selected in this system. The maximum net power and maximum power generation efficiency of the system with a fuel cell operating temperature of 800°C are 899.93 W and 52.52%, respectively.

The impact of the three key operating parameters and energy analysis provides a more comprehensive understanding of the performance and energy consumption distribution of the SOFC system for methane steam reforming to produce hydrogen, which can further optimize the SOFC-based power generation energy system to provide theoretical guidance.

Acknowledgements

This research has been supported by the National Natural Science Foundation of China (Grant No. 51866001) and Initial Research Funds for the Hainan Universities (KYQD(ZR)1841).

References

[1] Meng Q., Han J., Kong L., Liu H., et al., Thermodynamic analysis of combined power generation system based on SOFC/GT and transcritical carbon dioxide cycle. International Journal of Hydrogen Energy, 2017, 42: 4673–4678.

[2] Tan L.Z., Dong X.M., Gong Z.Q., et al., Investigation on performance of an integrated SOFC-GE-KC power generation system using gaseous fuel from biomass gasification. Renewable Energy, 2017, 107: 448–461.

[3] Heng W.G., Zhao H.B., Zhao Z.F., Thermodynamic performance study of a new SOFC-CCHP system with diesel reforming by CLHG to produce hydrogen as fuel. International Journal of Hydrogen Energy, 2021, 46: 22956–22973.

[4] Yan Z.Q., Zhao P., Wang J.F., et al., Thermodynamic

analysis of an SOFC-GT-ORC integrated power system with liquefied natural gas as heat sink. International Journal of Hydrogen Energy, 2013, 38: 3352–3363.

[5] Chatrattanawet N., Saebea D., Authayanun S., et al., Performance and environmental study of a biogas-fuelled solid oxide fuel cell with different reforming approaches. Energy, 2018, 146: 131–140.

[6] Chen X.Y., Wang C., Luo X.L., et al., Qualitative analysis of fluid dynamics and heat transfer characteristics in porous structures towards aqueous phase reforming hydrogen production. International Journal of Hydrogen Energy, 2021, 46: 23026–23039.

[7] Khani L., Mehr A.S., Yari M., et al., Multi-objective optimization of an indirectly integrated solid oxide fuel cell-gas turbine cogeneration system. International Journal of Hydrogen Energy, 2016, 41: 21470–21488.

[8] Safari A., Shahsavari H., Salehi J., A mathematical model of SOFC power plant for dynamic simulation of multi-machine power systems. Energy, 2018, 149: 397–413.

[9] Kupecki J., Motylinski K., Milewski J., Dynamic analysis of direct internal reforming in a SOFC stack with electrolyte-supported cells using a quasi-1D model. Applied Energy, 2018, 227: 198–205.

[10] Albrecht K.J., Braun R.J., The effect of coupled mass transport and internal reforming on modeling of solid oxide fuel cells part II: Benchmarking transient response and dynamic model fidelity assessment. Journal of Power Sources, 2016, 304: 402–408.

[11] Zhao Y.R., Sadhukhan J., Lanzini A., et al., Optimal integration strategies for a syngas fuelled SOFC and gas turbine hybrid. Journal of Power Sources, 2011, 196: 9516–9527.

[12] Chitgar N., Moghimi M., Design and evaluation of a novel multi-generation system based on SOFC-GT for electricity, fresh water and hydrogen production. Energy, 2020, 197: 117162.

[13] Atsonios K., Samlis C., Manou K., et al., Technical assessment of LNG based polygeneration systems for non-interconnected island cases using SOFC. International Journal of Hydrogen Energy, 2021, 46(6): 4827–4843.

[14] Hasan A., Dincer I., Assessment of an integrated gasification combined cycle using waste tires for hydrogen and fresh water production. International Journal of Hydrogen Energy, 2019, 44(36): 19730–19741.

[15] Singh R., Singh O., Comparative study of combined solid oxide fuel cell-gas turbine-Organic Rankine cycle for different working fluid in bottoming cycle. Energy Conversion and Management, 2018, 171: 659–670.

[16] Wang J.F., Yan Z.Q., Ma S.L., et al., Thermodynamic analysis of an integrated power generation system driven by solid oxide fuel cell. International Journal of Hydrogen Energy, 2012, 37(3): 2535–2545.

[17] Akkaya A.V., Sahin B., A study on performance of solid oxide fuel cell-organic Rankine cycle combined system. International Journal of Energy Research, 2009, 33(6): 553–564.

[18] Eisavi B., Chitsaz A., Hosseinpour J., et al., Thermo-environmental and economic comparison of three different arrangements of solid oxide fuel cell-gas turbine (SOFC-GT) hybrid systems. Energy Conversion and Management, 2018, 168: 343–356.

[19] Moradi M., Mehrpooya M., Optimal design and economic analysis of a hybrid solid oxide fuel cell and parabolic solar dish collector, combined cooling, heating and power (CCHP) system used for a large commercial tower. Energy, 2017, 130: 530–543.

[20] Kumar P., Singh O., Thermoeconomic analysis of SOFC-GT-VARS-ORC combined power and cooling system. International Journal of Hydrogen Energy, 2019, 44(50): 27575–27586.

[21] Mehdi M., Milad S., Ali Rahimi., et al., Technical performance analysis of a combined cooling heating and power (CCHP) system based on solid oxide fuel cell (SOFC) technology-A building application. Energy Conversion and Management, 2019, 198: 11176.

[22] Zhang X.S., Chen Z.W., Chen Z.B., et al., Exergy analysis of a novel chemical looping hydrogen generation system integrated with SOFC. Journal of Thermal Science, 2021, 30: 313–323.

[23] Biert V.L., Visser K., Aravind P.V., A comparison of steam reforming concepts in solid oxide fuel cell systems. Applied Energy, 2020, 264: 114748.

[24] Biert V.L., Godjevac M., Visser K., et al., Dynamic modelling of a direct internal reforming solid oxide fuel cell stack based on single cell experiments. Applied Energy, 2019, 250: 976–990.

[25] Zeng Z.Z., Qian Y.P., Zhang Y.J., et al., A review of heat transfer and thermal management methods for temperature gradient reduction in solid oxide fuel cell (SOFC) stacks. Applied Energy, 2020, 280: 115899.

[26] Powell M., Meinhardt K., Sprenkle V., et al., Demonstration of a highly efficient solid oxide fuel cell power system using adiabatic steam reforming and anode gas recirculation. Journal of Power Sources, 2012, 205: 377–384.

[27] Barelli L., Bidini G., Cinti G., et al., SOFC stack coupled with dry reforming. Applied Energy, 2017, 192: 498–507.

[28] Shiratori Y., Ogura T., Nakajima H., et al., Study on paper-structured catalyst for direct internal reforming SOFC fueled by the mixture of CH_4 and CO_2. International Journal of Hydrogen Energy, 2013, 38(25): 10542–10551.

[29] Saebea D., Authayanun S., Patcharavorachot Y., et al.,

Use of different renewable fuels in a steam reformer integrated into a solid oxide fuel cell: Theoretical analysis and performance comparison. Energy, 2013, 51: 305–313.

[30] Farhad S., Hamdullahpur F., Yoo Y., Performance evaluation of different configurations of biogas-fueled SOFC micro-CHP systems for residential applications. International Journal of Hydrogen Energy, 2010, 35(8): 3758–3768.

[31] Ding X.Y., Lv X.J., Weng Y.W., Performance study on intermediate temperature solid oxide fuel cell and gas turbine hybrid system fueled with wood chip gasified gas. Proceedings of the Chinese Society of Electrical Engineering, 2015, 35: 133–141.

[32] Liese E.A., Gemmen R.S., Performance comparison of internal reforming against external reforming in a solid oxide fuel cell, gas turbine hybrid system. Journal of Engineering for Gas Turbines and Power, 2005, 127(1): 86–90.

[33] Cocco D., Tola V., Externally reformed solid oxide fuel cell-micro-gas turbine (SOFC-MGT) hybrid systems fueled by methanol and di-methyl-ether (DME). Energy, 2009, 34(12): 2124–2130.

[34] Chitsaz A., Sadeghi M., Sadeghi M., et al., Exergoenvironmental comparison of internal reforming against external reforming in a cogeneration system based on solid oxide fuel cell using an evolutionary algorithm. Energy, 2018, 144: 420–431.

[35] Lee T.S., Chung J.N., Chen Y.C., Design and optimization of a combined fuel reforming and solid oxide fuel cell system with anode off-gas recycling. Energy Conversion and Management, 2011, 52(10): 3214–3226.

[36] Saebea D., Magistri L., Massardo A., et al., Cycle analysis of solid oxide fuel cell-gas turbine hybrid systems integrated ethanol steam reformer: Energy management. Energy, 2017, 127: 743–755.

[37] Chen B., Xu H.R., Zhang Y., et al., Combined methane reforming by carbon dioxide and steam in proton conducting solid oxide fuel cells for syngas/power co-generation. International Journal of Hydrogen Energy, 2019, 44(29): 15313–15321.

[38] Yuksel Y.E., Ozturk M., Dincer I., Development of a novel combined energy plant for multigeneration with hydrogen and ammonia production. International Journal of Hydrogen Energy, 2021, 46(57): 28980–28994.

[39] Koo T., Kim Y.S., Lee Y.D., et al., Exergetic evaluation of operation results of 5-kW-class SOFC-HCCI engine hybrid power generation system. Applied Energy, 2021, 295: 117037.

[40] Bessette N.F., Wepfer W., Winnick J., A mathematical model of a solid oxide fuel cell. Journal of the Electrochemical Society, 1995, 142: 3792.

[41] Mohammadnia A., Asadi A., A hybrid solid oxide fuel cell-gas turbine fed by the motive steam of a multi-effects desalination-thermo vapor compressor system. Energy Conversion and Management, 2020, 216: 112951.

[42] Ranjbar F., Chitsaz A., Mahmoudi S.M.S., et al., Energy and exergy assessments of a novel trigeneration system based on a solid oxide fuel cell. Energy Conversion and Management, 2014, 87: 318–327.

[43] Mahmoudi S.M.S., Khani L., Thermodynamic and exergoeconomic assessments of a new solid oxide fuel cell-gas turbine cogeneration system. Energy Conversion and Management, 2016, 123: 324–337.

[44] Ozcan H., Dincer I., Performance evaluation of an SOFC based trigeneration system using various gaseous fuels from biomass gasification. International Journal of Hydrogen Energy, 2015, 40(24): 7798–7807.

[45] Haseltalab A., Biert V.L., Sapra H., et al., Component sizing and energy management for SOFC-based ship power systems. Energy Conversion and Management, 2021, 245: 114625.

[46] Deng M.L, Zhang Q.W, Zhang X.S., et al., Integration and optimization for a PEMFC and PSA oxygen production combined system. Energy Conversion and Management, 2021, 236: 114062.

[47] Alirahmi S.M., Mousavi S.F., Ahmadi P., et al., Soft computing analysis of a compressed air energy storage and SOFC system via different artificial neural network architecture and tri-objective grey wolf optimization. Energy, 2021, 236: 121412.

[48] Corigliano O., Fragiacomo P., Extensive analysis of SOFC fed by direct syngas at different anodic compositions by using two numerical approaches. Energy Conversion and Management, 2020, 209: 112664.

[49] Calise F., d'Accadia M.D., Restuccia G., Simulation of a tubular solid oxide fuel cell through finite volume analysis: effects of the radiative heat transfer and exergy analysis. International Journal of Hydrogen Energy, 2007, 32(17): 4575–4590.

[50] Kupecki J., Papurello D., Lanzini A., et al., Numerical model of planar anode supported solid oxide fuel cell fed with fuel containing H_2S operated in direct internal reforming mode (DIR-SOFC). Applied Energy, 2018, 230: 1573–1584.

[51] Jia J.X., Li Q., Luo M., et al., Effects of gas recycle on performance of solid oxide fuel cell power systems. Energy, 2011, 36(2): 1068–1075.

[52] Gong Y.H., Huang K., Study of a renewable biomass fueled SOFC: The effect of catalysts. International Journal of Hydrogen Energy, 2013, 38(36): 16518–165 23.

[53] Fu Q.R., Li Z.Y., Wei W., et al., Performance enhancement of a beam and slot interconnector for anode-supported SOFC stack. Energy Conversion and

Management, 2021, 241: 114277.

[54] Lim T.H., Park J.L., Lee S.B., et al., Fabrication and operation of a 1 kW class anode-supported flat tubular SOFC stack. International Journal of Hydrogen Energy, 2010, 35(18): 9687–9692.

[55] Rosner F., Rao A., Samuelsen S., Economics of cell design and thermal management in solid oxide fuel cells under SOFC-GT hybrid operating conditions. Energy Conversion and Management, 2020, 220: 112952.

[56] Rosner F., Rao A., Samuelsen S., Thermo-economic analyses of solid oxide fuel cell-gas turbine hybrids considering thermal cell gradients. Journal of Power Sources, 2021, 507: 230271.

[57] Oryshchyn D., Harun N.F., Tucker D., et al., Fuel utilization effects on system efficiency in solid oxide fuel cell gas turbine hybrid systems. Applied Energy, 2018, 228: 1953–1965.

[58] Akkaya A.V., Sahin B., Huseyin E.H., Exergetic performance coefficient analysis of a simple fuel cell system. International Journal of Hydrogen Energy, 2007, 32(17): 4600–4609.

[59] Wu Z., Zhang Z.X., Ni M., Modeling of a novel SOFC-PEMFC hybrid system coupled with thermal swing adsorption for H_2 purification: Parametric and exergy analyses. Energy Conversion and Management, 2018, 174: 802–813.

[60] Sadeghi M., Jafari M., Hajimolana Y.S., et al., Size and exergy assessment of solid oxide fuel cell-based H_2-fed power generation system with alternative electrolytes: A comparative study. Energy Conversion and Management, 2021, 228: 113681.

[61] Rohini K.A., Lee H.J., Choi S.H., Numerical parametric study on the burner arrangement design for hydrogen production in a steam methane reformer. International Journal of Energy Research, 2021, 45(11): 16006–16026.

[62] Lv X.J., Gu C.H., Liu X., et al., Effect of gasified biomass fuel on load characteristics of an intermediate-temperature solid oxide fuel cell and gas turbine hybrid system. International Journal of Hydrogen Energy, 2016, 41(22): 9563–9576.

[63] Pan M.Z., Zhang K., Li X.Y., Optimization of supercritical carbon dioxide based combined cycles for solid oxide fuel cell-gas turbine system: Energy, exergy, environmental and economic analyses. Energy Conversion and Management, 2021, 248: 114774.

[64] Ding X.Y., Lv X.J., Weng Y.W., Coupling effect of operating parameters on performance of a biogas-fueled solid oxide fuel cell/gas turbine hybrid system. Applied Energy, 2019, 254: 113675.

[65] Wang Z.X., Mao J.K., He Z.Z., et al., Energy-exergy analysis of an integrated small-scale LT-PEMFC based on steam methane reforming process. Energy Conversion and Management, 2021, 246: 114685.

[66] Tacchino V., Costamagna P., Rosellini S., et al., Multi-scale model of a top-fired steam methane reforming reactor and validation with industrial experimental data. Chemical Engineering Journal, 2021. 428: 131492.

[67] Mei S.X., Lu X.R., Zhu Y., et al., Thermodynamic assessment of a system configuration strategy for a cogeneration system combining SOFC, thermoelectric generator, and absorption heat pump. Applied Energy, 2021, 302: 117573.

[68] Liso V., Olesen A.C., Nielsen M.P., et al., Performance comparison between partial oxidation and methane steam reforming processes for solid oxide fuel cell (SOFC) micro combined heat and power (CHP) system. Energy, 2011, 36(7): 4216–4226.

[69] Wang X.S., Lv X.J., Weng Y.W., Performance analysis of a biogas-fueled SOFC/GT hybrid system integrated with anode-combustor exhaust gas recirculation loops. Energy, 2020, 197: 117213.